[65] Bounhar, Y; Zhang, Y; Goodyer, CG and LeBlanc, A. Prion protein protects human neurons against Bax-mediated apoptosis. *J Biol Chem*, 2001 276, 39145-9

[66] Pisani, A; Bonsi, P and Calabresi, P. Calcium signaling and neuronal vulnerability to ischemia in the striatum. *Cell Calcium*, 2004 36, 277-84

[67] Colling, SB; Collinge, J and Jefferys, JG. Hippocampal slices from prion protein null mice: disrupted Ca(2+)-activated K+ currents. *Neurosci Lett*, 1996 209, 49-52

[68] Herms, JW; Korte, S; Gall, S; Schneider, I; Dunker, S and Kretzschmar, HA. Altered intracellular calcium homeostasis in cerebellar granule cells of prion protein-deficient mice. *J Neurochem*, 2000 75, 1487-92

[69] DeArmond, SJ and Prusiner, SB. Etiology and pathogenesis of prion diseases. *Am J Pathol*, 1995 146, 785-811

[70] Yokoyama, T; Kimura, KM; Ushiki, Y; Yamada, S; Morooka, A; Nakashiba, T; Sassa, T and Itohara, S. In vivo conversion of cellular prion protein to pathogenic isoforms, as monitored by conformation-specific antibodies. *J Biol Chem*, 2001 276, 11265-71

[71] Kitamoto, T; Amano, N; Terao, Y; Nakazato, Y; Isshiki, T; Mizutani, T and Tateishi, J. A new inherited prion disease (PrP-P105L mutation) showing spastic paraparesis. *Ann Neurol*, 1993 34, 808-13

[72] Neufeld, MY; Josiphov, J and Korczyn, AD. Demyelinating peripheral neuropathy in Creutzfeldt-Jakob disease. *Muscle Nerve*, 1992 15, 1234-9

[73] Tuzi, NL; Gall, E; Melton, D and Manson, JC. Expression of doppel in the CNS of mice does not modulate transmissible spongiform encephalopathy disease. *J Gen Virol*, 2002 83, 705-11

[74] Forloni, G; Angeretti, N; Chiesa, R; Monzani, E; Salmona, M; Bugiani, O and Tagliavini, F. Neurotoxicity of a prion protein fragment. *Nature*, 1993 362, 543-6

[75] Chen, SG; Teplow, DB; Parchi, P; Teller, JK; Gambetti, P and Autilio-Gambetti, L. Truncated forms of the human prion protein in normal brain and in prion diseases. *J Biol Chem*, 1995 270, 19173-80

Laboratory Investigation (2004) 84, 828–835

www.laboratoryinvestigation.org

Accumulation of prion protein in muscle fibers of experimental chloroquine myopathy: *in vivo* model for deposition of prion protein in non-neuronal tissues

Hisako Furukawa*, Katsumi Doh-ura†, Kensuke Sasaki and Toru Iwaki

Department of Neuropathology, Neurological Institute, Graduate School of Medical Sciences, Kyushu University, Fukuoka, Japan

Prion protein (PrP) is known to accumulate in some non-neuronal tissues under conditions unrelated to prion diseases. The biochemical and biological nature of such accumulated PrP molecules, however, has not been fully evaluated. In this study, we established experimental myopathy in hamsters by long-term administration of chloroquine, and we examined the nature of the PrP molecules that accumulated. PrP accumulation was immunohistochemically demonstrated in autophagic vacuoles in degenerated muscle fibers, and this was accompanied by the accumulation of other molecules related to the neuropathogenesis of prion diseases such as clathrin, cathepsin B, heparan sulfate, and apolipoprotein J. Accumulated PrP molecules were partially insoluble in detergent solution and were slightly less sensitive to proteinase K digestion than normal cellular PrP. Muscle homogenates containing these PrP molecules did not cause disease in inoculated hamsters. The findings indicate that the PrP molecules that accumulated in muscle fibers have distinct biochemical and biological properties. Therefore, experimental chloroquine myopathy is a novel and useful model to investigate the mechanism of deposition of PrP in non-neuronal tissues and might provide new insights in the pathogenesis of prion diseases.
Laboratory Investigation (2004) **84,** 828–835, advance online publication, 3 May 2004; doi:10.1038/labinvest.3700111

Keywords: detergent-solubility; experimental chloroquine myopathy; lysosome; non-neuronal tissues; prion protein; protease sensitivity

Prion diseases such as Creutzfeldt–Jakob disease in humans, and scrapie and bovine spongiform encephalopathy in animals are neurodegenerative disorders characterized by the accumulation in the brain of a protease-resistant, detergent-insoluble abnormal isoform of prion protein (PrP). This abnormal isoform of PrP (PrP^{Sc}) is pathogenic itself and replicates by altering the conformation of a protease-sensitive, detergent-soluble normal cellular isoform of prion protein (PrP^{C}).[1] In addition to the central nervous system, PrP^{Sc} deposition is observed in non-neuronal tissue such as tonsils and skeletal muscles in human prion diseases[2,3] and experimental animals.[4]

PrP is also known to accumulate in non-neuronal tissues under certain pathological conditions unrelated to prion diseases. Frederiske *et al*[5] recently revealed increased PrP immunoreactivity in the regions of fiber-cell degeneration in cataractous lenses in humans. Askanas *et al*[6] reported the accumulation of PrP in vacuolated muscle fibers, in angulated and round atrophic fibers with sarcolemmal enhancement, and in the perivascular inflammatory cells of sporadic inclusion-body myositis in humans.[6,7] It was also reported that the accumulated PrP molecules were sensitive to protease treatment.[7] However, the biochemical and biological characteristics of these PrP molecules have not been fully evaluated.

Chloroquine, a widely used antimalarial agent, is known to be concentrated in lysosomes and to cause elevation of intralysosomal pH.[8] Long-term

Correspondence: Dr H Furukawa, MD, PhD, Department of Pharmacology 1, Nagasaki University Graduate School of Biomedical Sciences, 1-12-4 Sakamoto, Nagasaki 852-8523, Japan.
E-mail: hisako@net.nagasaki-u.ac.jp
*Current address: Department of Pharmacology 1, Nagasaki University Graduate School of Biomedical Sciences, 1-12-4 Sakamoto, Nagasaki 852-8523, Japan.
†Division of Prion Protein Biology, Department of Prion Research, Tohoku University Graduate School of Medicine, 2-1 Seiryo-cho, Aoba-ku, Sendai 980-8575, Japan.
Received 16 January 2004; revised 7 March 2004; accepted 12 March 2004; published online 3 May 2004

administration of chloroquine sometimes causes myopathy, termed chloroquine myopathy (CM), which is characterized by degenerated muscle fibers with numerous autophagic, rimmed vacuoles.[9] Tsuzuki *et al*[10] established experimental CM in the rat to investigate the mechanism of accumulation of the proteins related to Alzheimer's disease in rimmed vacuoles, because of its histopathological similarity to human myopathies where amyloid β deposition is observed in rimmed vacuoles.

To explore the biochemical and biological properties of PrP molecules that accumulate under pathological conditions unrelated to prion diseases, we established experimental CM in hamsters and characterized the PrP molecules (PrP^{CQ}) that accumulated in affected muscle fibers.

Materials and methods

Animals and Reagents

Female Syrian hamsters, 3–8-week old, were purchased from SLC (Hamamatsu, Japan). Chloroquine diphosphate and Nonidet P-40 (NP-40) were purchased from Sigma Chemical (MO, USA). Proteinase K (PK) and complete mini protease inhibitor cocktail were obtained from Roche Molecular Biochemicals (Germany). Monoclonal antibody 3F4 recognizing hamster PrP109-112 was from Senetek (St Louis, MO, USA). Anti-prion protein polyclonal antibody PrP2B was raised by immunization of rabbits with a hamster PrP89-103 fragment. Polyclonal antibodies for apolipoprotein J (clusterin) and for cathepsin B, and monoclonal antibodies CHC5.9 for clathrin and HepSS-1 for heparan sulfate were purchased from Chemicon (Temecula, CA, USA), Calbiochem (Cambridge, MA, USA), PROGEN Biotechnik GmbH (Germany), and Seikagaku Corporation (Japan), respectively.

Experimental CM in Hamsters

Hamsters received 50 mg/kg chloroquine diphosphate (10 mg/ml in sterile saline, pH 7.6) as daily intraperitoneal injections for 60 days. Then the hamsters were killed by decapitation under deep anesthesia. Bilateral soleus, tibialis anterior, and quadriceps muscles were removed and immediately snap-frozen in isopentane cooled with liquid nitrogen. Frozen muscles were kept at −80°C until analysis.

Immunohistochemical Studies

After the blockage of endogenous peroxidase with 0.3% hydrogen peroxide in methanol, serial 10-μm thick sections of frozen muscle were incubated overnight at 4°C with the primary antibodies diluted with 10 mM phosphate-buffered saline (PBS) containing 1% normal hamster serum. The sections were then incubated with horseradish peroxidase-conjugated secondary antibodies for 1 h followed by reactions with 3,3′-diaminobenzidine/H_2O_2 and counterstained with hematoxylin. The serial sections were stained with hematoxylin and eosin (HE), or stained for acid phosphatase or by a modified Gomori-trichrome method.

Brain specimens obtained in some experiments were immersion-fixed in 10% buffered formalin for 24 h at 4°C and embedded in paraffin for immunohistochemical examination. For detection of abnormal PrP deposition, deparaffinized 8-μm thick sections were treated with hydrolytic autoclaving prior to incubation with 3F4 monoclonal antibody.[11]

Protease Sensitivity Assay of PrP^{CQ}

After confirmation of the histological findings, the remaining frozen muscle was homogenized using Tissue-Tearor (Biospec Products, Oklahoma) in 10 volumes of lysis buffer A (0.5% NP-40, 0.5% sodium deoxycholate in PBS pH 7.4). Homogenates were centrifuged at $3300 \times g$ for 15 min to remove the nuclear fraction and debris. The supernatant was then treated with the indicated amount of PK at 37°C for 20 min. After stopping the digestion with 4 mM 4-[2-aminoethyl]-benzenesulfonyl fluoride (Pefabloc, Roche, Germany), an aliquot corresponding to 4 mg of muscle tissue was analyzed by Western blotting using polyclonal antibody PrP2B. Labeled PrP was visualized by using CDP-star detection reagent (Amersham, UK).

Detergent Solubility Assay of PrP^{CQ}

The detergent solubility of PrP^{CQ} was determined as described by Lehmann and Harris[12] with minor modification. Briefly, soleus muscle samples from either control or CM hamsters were homogenized in lysis buffer B (15 mM NaCl, 50 mM Tris-HCl pH 7.5, complete-mini protease inhibitor cocktail) containing the designated concentration of NP-40. Homogenate was centrifuged for 5 min at 1600 *g* to remove debris and the nuclear fraction. The supernatant was ultracentrifuged at 265 000 *g* for 40 min at 25°C. Proteins in the supernatant and in the pellet were separately recovered and analyzed by Western blotting using monoclonal antibody 3F4.

Intracerebral Inoculation of PrP^{CQ}

Inoculum was prepared by homogenizing muscular tissue from CM hamsters or the control in 10 volumes of sterile saline, and 20 μl of the inoculum was injected into the brain of 19 3-week-old female hamsters under deep anesthesia. The hamsters were observed for over 2 years and killed to examine PrP molecules in the brain immunohistochemically.

Densitometry and Statistical Analysis

Blots of the gels were scanned with a CanoScan D2400UF (Canon, Japan). Densities of bands were quantified using NIH Image software. Statistical significance of densitometric data was analyzed by repeated measure ANOVA, and statistical comparison at each dose point between groups was made by Student's *t*-test or Welch's *t*-test.

Ethics

Animal handling and killing were in accordance with the nationally prescribed guidelines, with ethical approval for the study granted by the Animal Experiment Committee of Kyushu University.

Results

Histochemical Findings of CM

All the muscle specimens taken from chloroquine-treated hamsters showed various degrees of myopathic changes accompanied with rimmed vacuoles (Figure 1a), and this was consistent with histopathological findings of experimental CM in the rat.[9,10] In addition to the rimmed vacuoles, many muscle fibers contained coarse granular structures that were strongly stained by hematoxylin (Figure 1c) and modified Gomori trichrome stain (Figure 1g), and they showed enhanced acid phosphatase activity (Figure 1h). These abnormal structures were observed in about 10% of muscle fibers in the soleus muscle which was the most affected in all the muscles of chloroquine-treated hamsters. In contrast, muscles of control hamsters did not contain any rimmed vacuoles or coarse granular structures.

All of the rimmed vacuoles and the coarsely granular structures in degenerated muscle fibers of CM were positively stained by an anti-PrP monoclonal antibody, 3F4, recognizing hamster PrP109-112 (Figure 1b, d). In control hamster muscles, the 3F4 monoclonal antibody reacted with sarcolemmal membranes (data not shown).

To investigate the possible involvement of some molecules that relate to the metabolism of PrP^{C} or the deposition of PrP^{Sc}, serial sections were immunostained for apolipoprotein J (Figure 1e), clathrin (Figure 1f), cathepsin B (Figure 1i), and heparan sulfate (Figure 1j). Immunoreactivities for these molecules were enhanced in the rimmed vacuoles and coarse granular structures in the affected muscle fibers of CM.

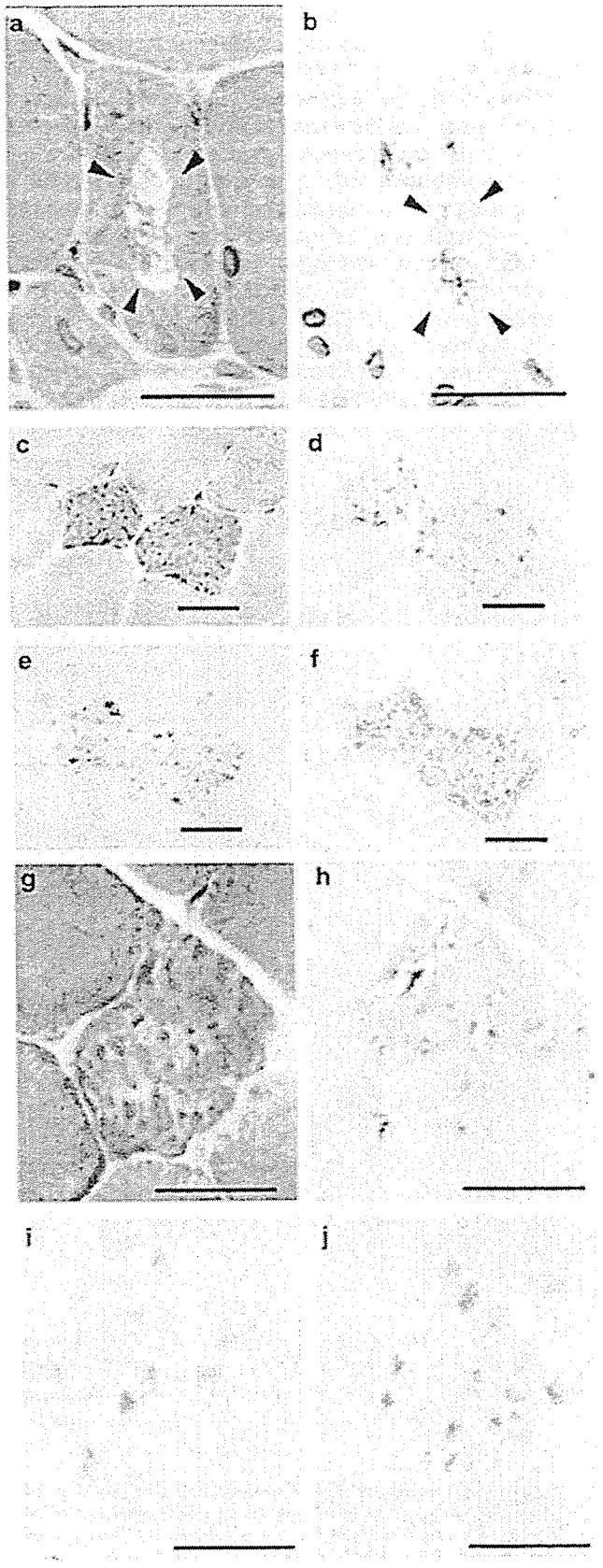

Figure 1 Immunohistochemical findings in CM muscles. Transverse sections of chloroquine-treated (50 mg/kg/day for 60 days) hamster soleus muscles are shown. (**a**) HE stain shows rimmed vacuole formation (arrow heads). (**b**) Immunoreactivity for PrP is detected in a rimmed vacuole (arrow heads) shown in (**a**). (**c–f**), (**g–j**) Serial sections stained with HE (**c**), modified Gomori trichrome (**g**), acid phosphatase (**h**), and immunostained for PrP (**d**), apolipoprotein J (**e**), clathrin (**f**), cathepsin B (**i**), and heparan sulfate (**j**). Scale bars = 20 μm.

PrP^{CQ} is Slightly Less Sensitive to PK Digestion

Western blot analysis using a polyclonal antibody PrP2B, raised against hamster PrP89-103, revealed prominent bands of 27 and 30 kDa in either CM muscular homogenates or the control, before digestion with PK. There was no significant difference in the intensity of PrP signals between CM muscles and controls (first lanes, Figure 2a, b). The specificity of these bands was confirmed by absorbing the PrP2B antibody with synthetic peptide PrP89-103 (Figure 2c). Although both of the PrP molecules were completely digested with 50 μg/ml of PK, which was the stringent condition to distinguish PrP^{Sc} from PrP^{C} (data not shown), digestion with a smaller amount of PK revealed different PK sensitivity between the PrP molecules from CM muscles (PrP^{CQ}) and PrP^{C} from the control muscles. PrP^{C} derived from control hamster muscle was apparently digested with 0.375 μg/ml of PK, whereas a considerable amount of PrP^{CQ} of 27 kDa still remained after treatment with 1.0 μg/ml of PK (Figure 2a and b). Statistical analysis of the relative density of the bands revealed a significant difference between PrP^{C} and PrP^{CQ} after treatment with 0.5, 0.75, or 1.0 μg/ml of PK (Figure 2d).

PrP^{CQ} is Partially Insoluble in Detergent

Western blot analysis using a monoclonal antibody 3F4 revealed prominent signals at 35 kDa and additional signals at about 30 kDa in the supernatants from either CM muscle homogenate or the control (first lanes, Figure 3a, b). While PrP^{C} from control muscle was completely solubilized in the lysis buffer containing 0.5% NP-40 (Figure 3a), a considerable amount of PrP^{CQ} remained in the

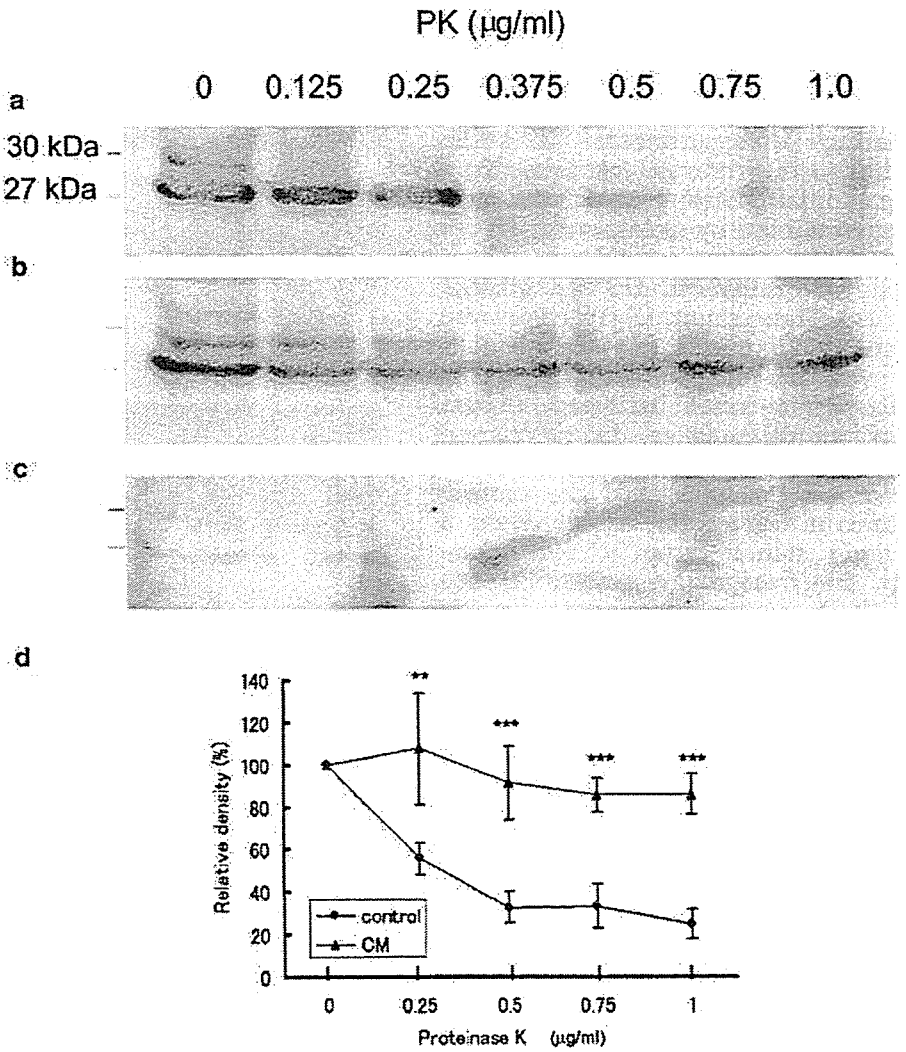

Figure 2 PK sensitivity of PrP molecules in CM muscles. (a–c) PrP molecules in the homogenate of control hamsters (a) or CM hamsters (b) were detected with PrP2B antibody after digestion with a designated amounts of PK at 37°C for 20 min. Prominent bands of 27 kDa and 30 kDa were diminished after the antibody had been absorbed by a synthetic polypeptide used for immunization (c). (d) Densitometric analysis of 27 and 30 kDa bands. Data from three independent experiments are indicated. $^{**}P<0.05$, $^{***}P<0.01$.

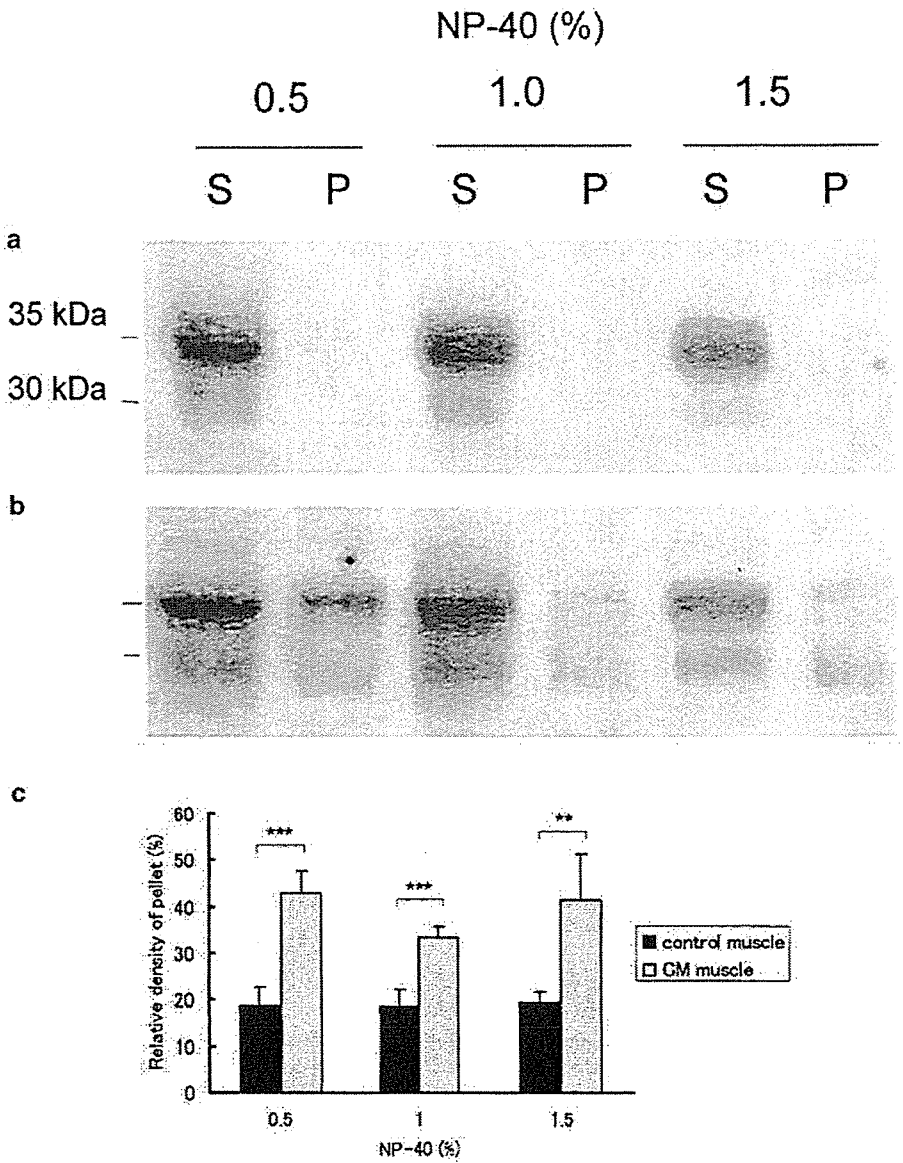

Figure 3 Solubility in NP-40 of PrP molecules in CM muscles. (**a**, **b**) Muscles from control hamsters (**a**) or CM hamsters (**b**) were homogenized in the lysis buffer containing designated amount of NP-40 and subsequently ultracentrifuged at 265 000 *g* to separate detergent-soluble PrP molecules in the supernatant (S) and detergent-insoluble molecules in the pellet (P). PrP molecules were labeled with 3F4 monoclonal antibody. (**c**) Relative PrP amount in the pellet fraction. Percentage of PrP signals (30 and 35 kDa) of the pellet fraction in the sum of those of the pellet and the supernatant is shown. Data from three independent experiments. $^{**}P<0.05$, $^{***}P<0.01$.

insoluble fraction in the presence of 0.5, 1.0, or 1.5% NP-40 (Figure 3b, c).

PrP^{CQ} is not Pathogenic

To investigate whether PrP^{CQ} is able to cause pathological changes characteristic of prion diseases *in vivo*, 10% muscular homogenates containing PrP^{CQ} were injected into the brain of Syrian hamsters. The hamsters were observed over 2 years after the inoculation had been given, and none of them developed any signs of prion diseases nor muscle disorders (data not shown). Histological examination of the brain revealed no significant pathological findings or abnormal PrP deposition (Figure 4).

Discussion

In this study, we have demonstrated that slightly less PK-sensitive and partially detergent-insoluble PrP^{CQ} accumulated in affected muscle fibers of experimental CM in hamsters. While PrP molecules from control muscle were sensitive to PK digestion at 0.375 μg/ml and fully soluble in buffer containing 0.5% NP-40, PrP^{CQ} molecules were less sensitive to PK digestion up to 1.0 μg/ml, and a considerable portion of them was insoluble in buffer containing

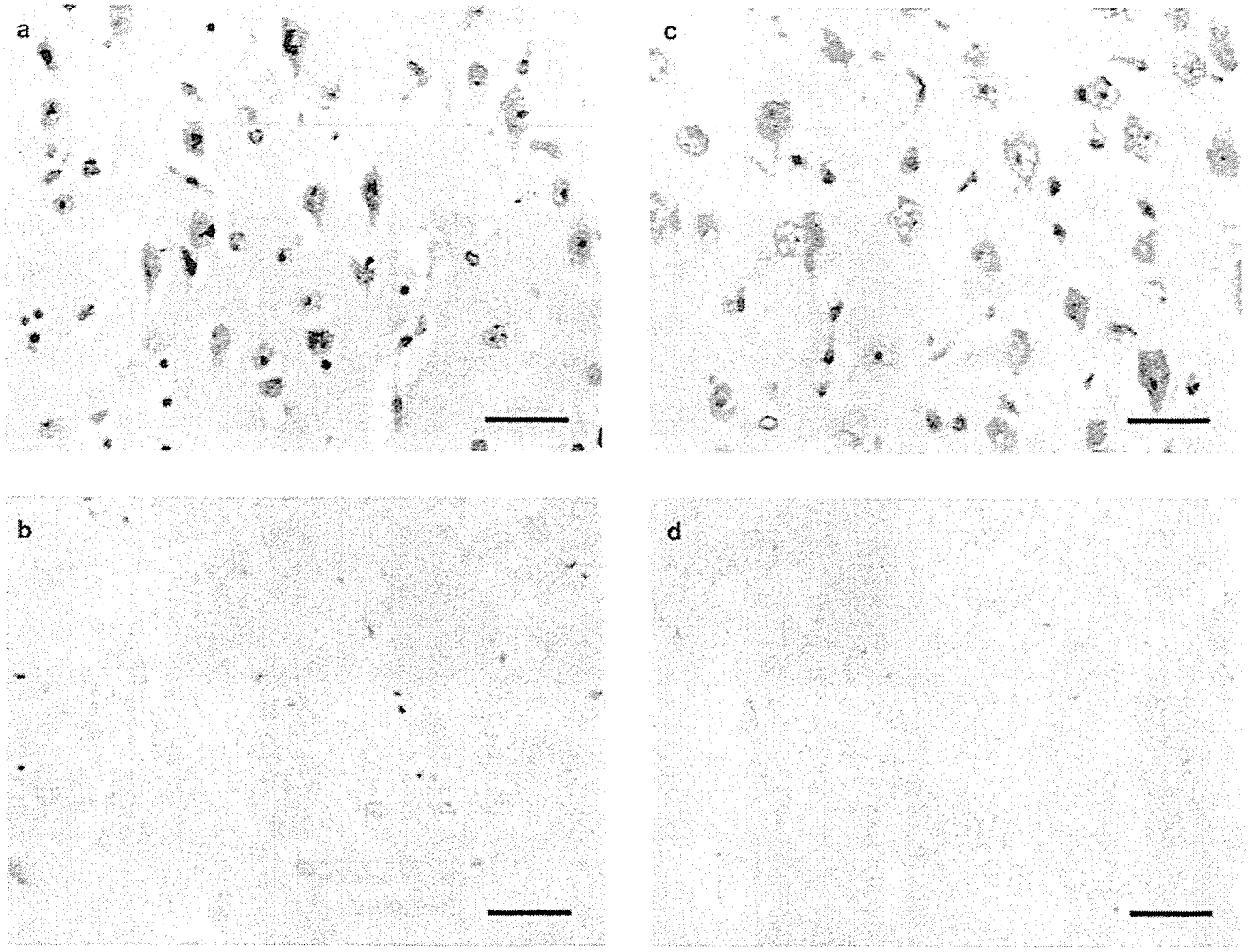

Figure 4 Histological analysis of hamster brain inoculated with CM muscle homogenate. Sections of the brain inoculated with PrP^{C}-containing muscle homogenate (**a**, **b**) or PrP^{CQ}-containing muscle homogenate (**c**, **d**) were stained with HE (**a**, **c**) or immunostained using 3F4 monoclonal antibody (**b**, **d**). Neither neurodegenerative change nor abnormal PrP deposition was revealed. Scale bars = 30 μm.

1.5% NP-40. These biochemical properties of PrP^{CQ} molecules are distinct from PrP^{C}.

There have been several attempts to create *de novo* PrP^{Sc}-like molecules *in vitro*. Using a cell-free conversion system, Horiuchi *et al*[13] were able to convert PrP^{C} into a protease-resistant isoform by the addition of PrP^{Sc} under physiological conditions. Even in the absence of PrP^{Sc}, an acidic buffer can give a β-sheet-dominant conformation and PK resistance to PrP^{C} *in vitro*.[14,15] Nevertheless, no *de novo* PrP^{Sc}-like molecules succeeded to reproduce the disease *in vivo*.[16] In the present study, PrP^{CQ} molecules were not capable of causing any pathological changes in the central nervous system. PrP^{CQ} molecules seem to be distinct from both of these *de novo* PrP^{Sc}-like molecules and PrP^{Sc}, because PrP^{CQ} molecules possess neither marked resistance to PK and detergent insolubility nor transmissibility of the disease conditions.

The CM model reported in this study is different from other PrP-conversion models previously reported, in that PrP^{CQ} molecule was generated *in vivo* in the absence of exogenous input of PrP^{Sc} or PrP^{Sc}-like molecules. Instead, the microenvironment in the lysosome was altered in hamsters by the injection of chloroquine to produce this distinct PrP molecule. Lysosomes are acidic compartments that have been reported to play an important role in the conformational conversion of PrP in prion diseases.[17,18] Chloroquine raises intralysosomal pH to as high as 6.0–6.5, causing marked changes in intracellular protein processing and trafficking.[8] As a consequence of the long-term administration of chloroquine, skeletal muscle fibers degenerate, with numerous autophagic vacuoles.[9] In the process of forming autophagic vacuoles, endogenous muscular PrP^{C} could acquire the properties of PrP^{CQ}.

In the present study, it remains unclear whether chloroquine modifies PrP^{C} molecules directly or indirectly. A previous study revealed that chloroquine does not directly interact with PrP molecules in scrapie-infected neuroblastoma cells.[19]

Furthermore, it has been reported that unfolded recombinant human prion protein PrP90-231 forms a stable protein folding intermediate rich in β-sheet at pH lower than 4.[14] Matsunaga *et al*[20] reported that pH is a crucial factor in determining the conformational state of some amyloidgenic proteins. They found that synthetic Aβ42 and stefin B peptides, showing similar amino-acid alignment to PrP90-144, tend to form amyloid fibrils at acidic pH. Considering these observations, it is unlikely that chloroquine directly interacts with PrP^{C} molecules. An increase in lysosomal pH due to chloroquine, and subsequent metabolic changes in lysosomal systems might be responsible for the biosynthesis of PrP^{CQ} molecules.

Besides experimental CM, there are a few experimental models in which PrP molecules of skeletal muscle are rendered partially PK-resistant and detergent-insoluble. Chiesa *et al*[21] established transgenic mice expressing PrP molecules with nine-octapeptide insertional mutation. Mutated PrP molecules obtained PrP^{Sc}-like properties in the brain and the periphery, producing neurodegeneration similar to an inherited prion disease in humans. In their model, the primary structure of PrP molecules was changed and the mutated PrP was overexpressed not only in the brain but also in the skeletal muscle and heart. This model is quite different from our CM model, in that the primary structure of PrP molecules was not manipulated.

The other experimental model is a transgenic mouse harboring high copy numbers of wild-type PrP transgenes, which spontaneously exhibited necrotizing myopathy, demyelinating polyneuropathy, and focal vacuolation of the central nervous system without apparent deposition of PrP^{Sc}.[22] In spite of severe neurodegeneration and neuromyopathy, only small amount of PK-resistant PrP was detected in affected muscles and brains. They concluded that low level of PK-resistant PrP might reflect aggregation of PrP^{C} and was not correlated with neuropathological changes in these transgenic mice. In our study, PrP^{CQ} after PK digestion did not show molecular characteristics of PrP^{Sc} in prion diseases, suggesting that PrP^{CQ} acquires less PK sensitivity through a different mechanism from that of PrP^{Sc}. Although the expression level of PrP was not increased in CM (data not shown), it is possible that distinct biochemical properties of PrP^{CQ} might simply be due to protein aggregation or alteration in PK–protein ratio, not to the conformational change of monomeric PrP^{C} molecules.

PrP^{CQ} in the affected muscles of the present model was accompanied by the accumulation not only of lysosomal markers but also of those molecules known to be involved in prion disease pathogenesis, such as clathrin, heparan sulfate proteoglycan, and apolipoprotein J.[23–25] It is known that certain sulfated glycans, such as heparan sulfate and pentosan polysulfate, stimulate PrP conversion *in vitro*.[26] Then, it might be possible that accumulated heparan sulfate in the CM muscles contribute to the acquisition of altered PK sensitivity and partial detergent insolubility of the PrP molecules.

Experimental CM in the rat has been established previously as a model of myopathies with rimmed vacuoles, including distal myopathy with rimmed vacuole formation and inclusion-body myositis. Owing to of the deposition of amyloid β in inclusion-body myositis,[27] experimental CM has been utilized by several groups as a peripheral model to investigate the pathogenesis of Alzheimer's disease.[10,28] The precise mechanism of rimmed vacuole formation in CM is still unknown; however, it has been reported that chloroquine causes an increase in endogenous autophagosomes in mammalian cells.[29] Similar mechanism(s) might be shared between amyloid β deposition in the CM rat model and PrP^{CQ} accumulation in our CM hamster model.

The PrP2B polyclonal antibody revealed prominent 27 kDa signals with additional 30 kDa signals (Figure 2), while the 3F4 monoclonal antibody reacted with dominant 35 kDa signals and additional 30 kDa signals (Figure 3), which were similar to Cp33-37 signal in skeletal muscle of hamster.[30] The common signals of 30 kDa were detected by both of the two antibodies. Minor epitope differences between the two antibodies might account for such a diversity of PrP signals, but it remains to be elucidated.

Finally, together with the biochemical and biological properties of PrP^{CQ}, the immunohistochemical findings in CM muscles of the molecules known to be involved in prion disease pathogenesis indicate that experimental CM in hamsters is a useful *in vivo* model to investigate the mechanism of PrP accumulation in the pathogenesis of PrP-related diseases.

Acknowledgements

We are grateful to Professor Mitsuo Takahashi at Fukuoka University and Professor Masami Niwa at Nagasaki University for their critique and suggestions on the research and this report. The English used in this manuscript was revised by Universal Academy Press, Inc., Japan.

This work was supported by a grant (H13-kokoro-025) to KD from the Ministry of Health, Labor and Welfare of Japan.

References

1 Prusiner SB. Molecular biology of prion diseases. Science 1991;252:1515–1522.
2 Hill AF, Zeidler M, Ironside J, *et al*. Diagnosis of new variant Creutzfeldt-Jakob disease by tonsil biopsy. Lancet 1997;349:99–100.
3 Glazel M, Abela E, Maisson M, *et al*. Extraneural pathologic prion protein in sporadic Creutzfeldt–Jakob disease. N Eng J Med 2003;349:1812–1820.

4 Bosque PJ, Ryou C, Telling G, *et al.* Prions in skeletal muscle. Proc Natl Acad Sci USA 2002;99:3812–3817.
5 Frederikse PH, Zigler Jr SJ, Farnsworth PN, *et al.* Prion protein expression in mammalian lenses. Curr Eye Res 2000;20:137–143.
6 Askanas V, Bilak M, Engel WK, *et al.* Prion protein is abnormally accumulated in inclusion-body myositis. Neuroreport 1993;5:25–28.
7 Zanusso G, Vattemi G, Ferrari S, *et al.* Increased expression of the normal cellular isoform of prion protein in inclusion-body myositis, inflammatory myopathies and denervation atrophy. Brain Pathol 2001;11:182–189.
8 Holzman E. Lysosomes. Cellular organelles. Plenum Press: New York and London, 1989.
9 Macdonald RD, Engel AG. Experimental chloroquine myopathy. J Neuropath Exp Neurol 1970;29:479–499.
10 Tsuzuki K, Fukatsu R, Takamaru Y, *et al.* Co-localization of amyloid-associated proteins with amyloid beta in rat soleus muscle in chloroquine-induced myopathy: a possible model for amyloid beta formation in Alzheimer's disease. Brain Res 1995;699:260–265.
11 Kitamoto T, Shin RW, Doh-ura K, *et al.* Abnormal isoform of prion protein accumulates in the synaptic structures of the central nervous system in patients with Creutzfeldt–Jakob disease. Am J Path 1992;140: 1285–1294.
12 Lehmann S, Harris DA. Blockade of glycosylation promotes acquisition of scrapie-like properties by the prion protein in cultured cells. J Biol Chem 1997; 272:21479–21487.
13 Horiuchi M, Caughey B. Specific binding of normal prion protein to the scrapie form via a localized domain initiates its conversion to the protease-resistant state. EMBO J 1999;18:3193–3203.
14 Swietnicki W, Peterson R, Gambetti P, *et al.* pH-dependent stability and conformation of the recombinant human prion protein PrP(90-231). J Biol Chem 1997;272:27517–27520.
15 Matsunaga Y, Peretz D, Williamson A, *et al.* Cryptic epitope in N-teminally truncated prion protein are exposed in the full-length molecule: dependence of conformation on pH. Proteins 2001;44:110–118.
16 Hill AF, Antoniou M, Collinge J. Protease-resistant prion protein produced *in vitro* lacks detectable infectivity. J Gen Virol 1999;80:11–14.
17 Laszlo L, Lowe J, Self T, *et al.* Lysosomes as key organelles in the pathogenesis of prion encephalopathies. J Pathol 1992;166:333–341.
18 Shyng SL, Huber MT, Harris DA. A prion protein cycles between the cell surface and an endocytic compartment in cultured neuroblastoma cells. J Biol Chem 1993;268:15922–15928.
19 Doh-ura K, Iwaki T, Caughey B. Lysosomotropic agents and cysteine protease inhibitors inhibit scrapie-associated prion protein accumulation. J Virol 2000;74:4894–4897.
20 Matsunaga Y, Zerovnik E, Yamada T, *et al.* Conformational changes preceding amyloid-fibril formation of amyloid-beta and stefin B: parallels in pH dependence. Curr Med Chem 2002;9:1717–1724.
21 Chiesa R, Pestronk A, Schmidt RE, *et al.* Primary myopathy and accumulation of PrPSc-like molecules in peripheral tissues of transgenic mice expressing a prion protein insertional mutation. Neurobiol Dis 2001;8:279–288.
22 Westaway D, DeArmond SJ, Cayetano-Canlas J, *et al.* Degeneration of skeletal muscle, peripheral nerves, and the central nervous system in transgenic mice overexpressing wild-type prion proteins. Cell 1994; 76:117–129.
23 Mouillet-Richard S, Ermonval M, Chebassier C, *et al.* Signal transduction through prion protein. Science 2000;289:1925–1928.
24 McBride PA, Wilson MI, Eikeleboom P, *et al.* Heparan sulfate proteoglycan is associated with amyloid plaques and neuroanatomically targeted PrP pathology throughout the incubation period of scrapie-infected mice. Exp Neurol 1998;149:447–454.
25 Sasaki K, Doh-ura K, Ironside JW, *et al.* Increased clusterin (apolipoprotein J) expression in human and mouse brains infected with transmissible spongiform encephalopathies. Acta Neuropathol (Berl) 2002;103: 199–208.
26 Wong C, Xiong LW, Horiuchi M, *et al.* Sulfated glycans and elevated temperature stimulate PrP^{Sc}-dependent cell-free formation of protease-resistant prion protein. EMBO J 2001;20:377–386.
27 Askanas V, Engel WK, Alvarez RB, *et al.* Beta-amyloid protein immunoreactivity in muscle of patients with inclusion-body myositis. Lancet 1992; 339:560–561.
28 Murakami N, Oyama F, Gu Y, *et al.* Accumulation of tau in autophagic vacuoles in chloroquine myopathy. J Neuropathol Exp Neurol 1998;57:664–673.
29 Suzuki T, Nakagawa M, Yoshikawa A, *et al.* The first molecular evidence that autophagy relates rimmed vacuole formation in chloroquine myopathy. J Biochem 2002;131:647–651.
30 Bendheim PE, Brown HR, Rudelli RD, *et al.* Nearly ubiquitous tissue distribution of the scrapie agent precursor protein. Neurology 1992;42:149–156.

JOURNAL OF VIROLOGY, May 2004, p. 4999–5006 Vol. 78, No. 10
0022-538X/04/$08.00+0 DOI: 10.1128/JVI.78.10.4999–5006.2004

Treatment of Transmissible Spongiform Encephalopathy by Intraventricular Drug Infusion in Animal Models

Katsumi Doh-ura,[1]* Kensuke Ishikawa,[1]† Ikuko Murakami-Kubo,[1] Kensuke Sasaki,[1] Shirou Mohri,[2] Richard Race,[3] and Toru Iwaki[1]

Department of Neuropathology[1] and Center of Biomedical Research,[2] Graduate School of Medical Sciences, Kyushu University, Fukuoka 812-8582, Japan, and Laboratory of Persistent Viral Diseases, Rocky Mountain Laboratories, National Institute of Allergy and Infectious Diseases, National Institutes of Health, Hamilton, Montana 59840[3]

Received 6 October 2003/Accepted 9 January 2004

The therapeutic efficacy of direct drug infusion into the brain, the target organ of transmissible spongiform encephalopathies, was assessed in transgenic mice intracerebrally infected with 263K scrapie agent. Pentosan polysulfate (PPS) gave the most dramatic prolongation of the incubation period, and amphotericin B had intermediate effects, but antimalarial drugs such as quinacrine gave no significant prolongation. Treatment with the highest dose of PPS at an early or late stage of the infection prolonged the incubation time by 2.4 or 1.7 times that of the control mice, respectively. PPS infusion decreased not only abnormal prion protein deposition but also neurodegenerative changes and infectivity. These alterations were observed within the brain hemisphere fitted with an intraventricular infusion cannula but not within the contralateral hemisphere, even at the terminal disease stage long after the infusion had ended. Therapeutic effects of PPS were also demonstrated in mice infected with either RML agent or Fukuoka-1 agent. However, at doses higher than that providing the maximal effects, intraventricular PPS infusion caused adverse effects such as hematoma formation in the experimental animals. These findings indicate that intraventricular PPS infusion might be useful for the treatment of transmissible spongiform encephalopathies in humans, providing that the therapeutic dosage is carefully evaluated.

Transmissible spongiform encephalopathies (TSEs), or prion diseases, are fatal neurodegenerative disorders that include Creuzfeldt-Jakob disease (CJD) and Gerstmann-Sträussler-Scheinker disease in humans, in addition to scrapie and bovine spongiform encephalopathy in animals. These disorders are characterized by deposition in the brain of a protease-resistant isoform of prion protein (PrP), which is thought to be the main pathogenic component responsible for the pathogenesis (18). Outbreaks of acquired forms of human TSEs, such as variant CJD (21) and iatrogenic CJD with cadaveric growth hormone or dura grafts (3) in younger people, are prompting the development of prophylactic and therapeutic interventions.

There are some chemicals that are effective in inhibiting the accumulation or conformational change of PrP molecules in vitro and/or in prolonging the incubation period when they are administered around the time of infection in TSE animal models (2, 17). However, no chemicals, except for amphotericin B and one of its derivatives, have been reported to improve prognosis when they are administered late in the disease course or after the infectious agent has already invaded the brain (8). This implies that it may be difficult to improve the prognosis in human patients by using chemicals, because patients first come to medical attention after the onset of neurological symptoms.

* Corresponding author. Present address: Department of Prion Research, Tohoku University Graduate School of Medicine, 2-1 Seiryo-cho, Aoba-ku, Sendai 980-8575, Japan. Phone: 81-22-717-8232. Fax: 81-22-717-8148. E-mail: doh-ura@mail.tains.tohoku.ac.jp.

† Present address: Department of Prion Research, Tohoku University Graduate School of Medicine, Sendai 980-8575, Japan.

Most of the previously reported chemicals have been large and hydrophilic, and whether their ineffectiveness was actually due to their poor accessibility to the brain has not been evaluated. We have developed a more sensitive drug evaluation system, which does not depend on drug accessibility to the brain, by implanting a continuous intraventricular drug infusion device into an intracerebrally TSE-infected animal model. Using this model, we have examined clinically applicable chemicals that have previously been reported to be effective either in vitro or in vivo, including antimalarial drugs such as quinacrine and chloroquine, the E-64d cysteine protease inhibitor, amphotericin B, and pentosan polysulfate (PPS). We report that intraventricular administration of PPS through the infusion device inhibited not only abnormal PrP accumulation but also neurodegenerative changes and infectivity in the brain, thereby giving rise to a dramatic prolongation of the life spans of intracerebrally infected animals.

MATERIALS AND METHODS

Experimental animals and in vivo evaluation. Tg7 mice, which are derived from Tg10 mice (19) and express hamster PrP but not endogenous mouse PrP, were inoculated with 20 μl of 1% 263K agent hamster homogenate in the right parietal portion of the brain. An Alzet osmotic pump (Durect, Cupertino, Calif.) filled with a chemical was placed in a subcutaneous area of the back. An intraventricular infusion cannula connected to the osmotic pump through a catheter was implanted in the left frontal portion of the brain in order to place the cannula tip into the left ventricle at either day 10 or 35 postinoculation or at another designated time. The pump worked stably from 40 h after implantation and continuously for 4 weeks. Five to 10 male mice per group, each weighing about 35 g, were used. Each mouse was kept in an individual cage under the same feeding and watering conditions in an air-conditioned, light time-controlled, specific-pathogen-free room. The mice began to exhibit ambiguous signs of reduced activity about 2 days prior to death, followed by obvious signs of ruffled

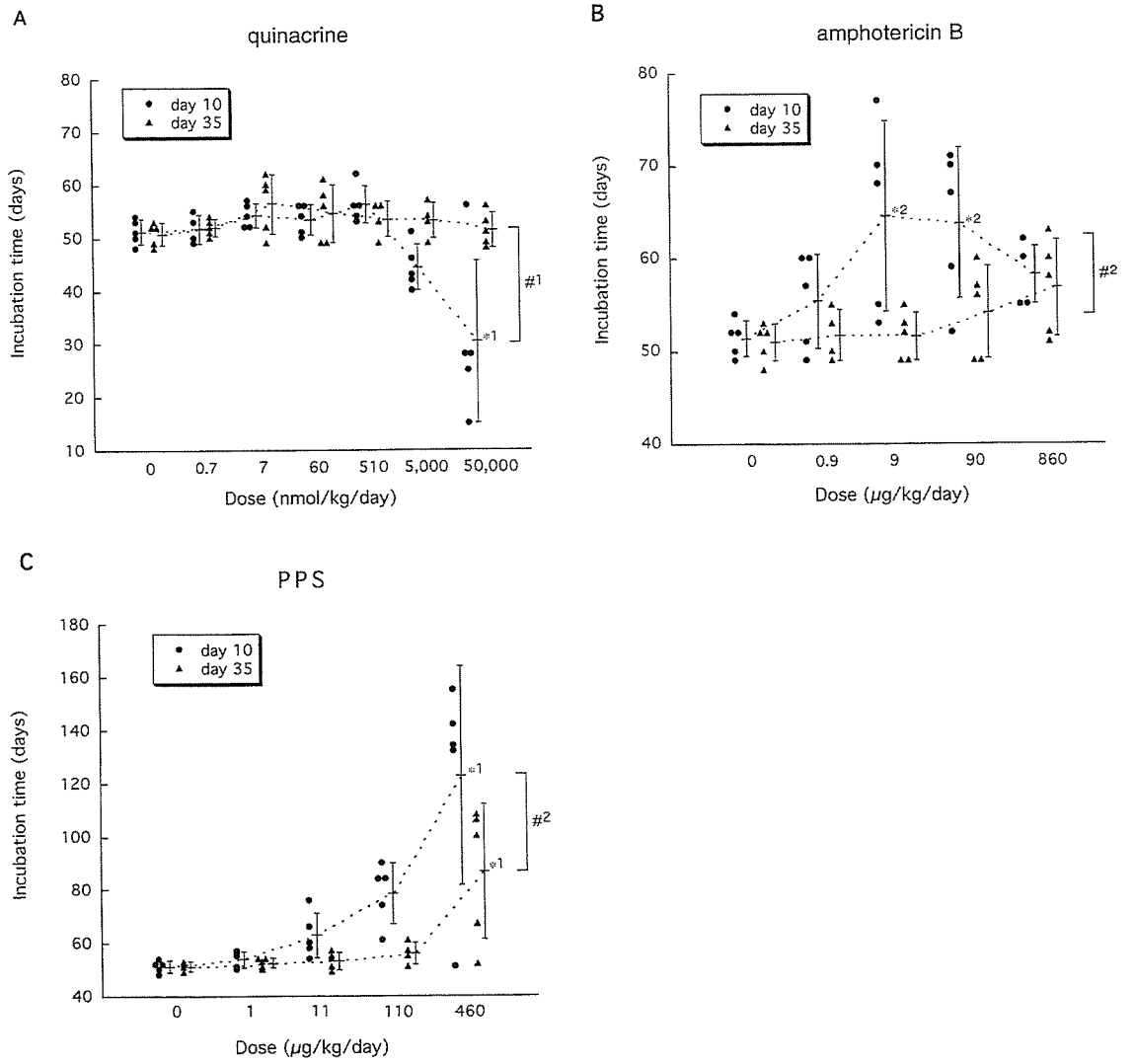

FIG. 1. Efficacy of quinacrine (A), amphotericin B (B), and PPS (C) in intracerebrally infected mice. Intraventricular infusion of a chemical was initiated at an early infection stage (day 10 postinoculation) or at a late stage (day 35) in 263K-infected Tg7 mice and continued for 4 weeks. Each circle or triangle represents an individual mouse. Bars represent the means and standard deviations of the incubation times for each group. *1, $P < 0.05$ versus the neighboring group and $P < 0.01$ versus the other groups; *2, $P < 0.05$ versus the vehicle control; #1, $P < 0.05$, #2, $P < 0.01$.

fur and bradykinesia on the day before or the day of death. The incubation period during which the animals were observed every day lasted from the time of intracerebral infection to the time of an obvious clinical stage.

Tga20 mice (14), which overexpress mouse PrP, were similarly inoculated with 1% RML agent mouse homogenate or 1% Fukuoka-1 agent mouse homogenate, and 4-week continuous intraventricular infusion of a chemical was started at day 14 or 49 postinoculation as described above.

Chemicals. The E-64d cysteine protease inhibitor was generously provided by S. Ishiura, Tokyo University, Tokyo, Japan. Quinacrine and chloroquine were obtained from Sigma. Amphotericin B (Fungizone) was purchased from Bristol-Myers Squibb (Tokyo, Japan). The sodium salt of PPS (Cartrophen Vet) was purchased from Biopharm (Bondi Junction, New South Wales, Australia) and used after removal of an alcohol additive by drying. E-64d was dissolved in dimethyl sulfoxide, amphotericin B was dissolved in distilled water, and all other chemicals were dissolved in phosphate-buffered saline (PBS).

Immunohistochemistry, immunoblotting, and infectivity assay. Mouse brains were fixed with 10% formalin and embedded in paraffin. Sections (5 μm thick) of the coronal slice sited around one-third of the distance from the interaural line to the bregma line were dewaxed and immunostained with an anti-PrP-C antibody (1:200; Immuno-Biological Labs, Gunma, Japan) or an antibody against glial fibrillary acidic protein (GFAP) (1:1,000; Dako, Glostrup, Denmark) as previously described (11).

For the detection of protease-resistant PrP (PrPres) by immunoblotting, the whole brain hemisphere where the intraventricular cannula had been fitted was homogenized with a ninefold volume of lysis buffer (0.5% sodium deoxycholate, 0.5% Nonidet P-40, PBS), and following low-speed centrifugation, the supernatant (Sup1) was treated with 25 μg of proteinase K per ml for 30 min at 37°C. An aliquot corresponding to 2.0 mg of brain tissue was electrophoresed in a sodium dodecyl sulfate–15% polyacrylamide gel and electroblotted onto a polyvinylidene difluoride filter. The filter was incubated with an anti-PrP-2B antibody raised against a hamster PrP fragment (amino acids 89 to 103) and then with an alkaline phosphatase-conjugated secondary antibody (Promega). Signals were visualized with CDP-Star detection reagent (Amersham).

For the infectivity assay, an aliquot of the Sup1 described above was diluted with PBS to produce a 0.1% brain homogenate, and a 20-μl aliquot of this homogenate was then inoculated intracerebrally in Tg7 mice. The infectious titer was calculated from the incubation period based on standard data obtained from an inoculation study with serially diluted homogenate samples of 263K-infected, terminally diseased brain tissue.

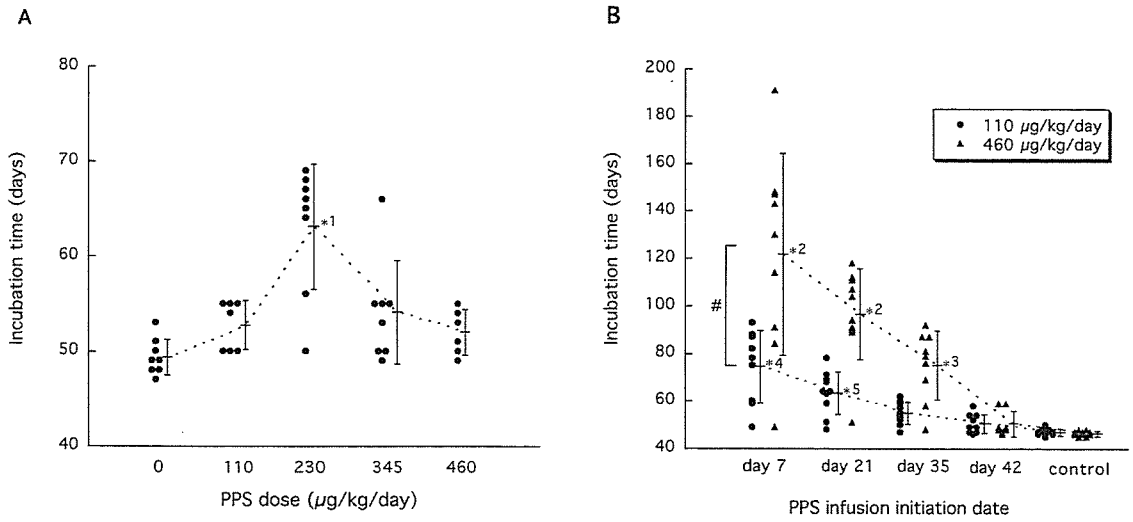

FIG. 2. Dose response (A) and administration timing (B) in PPS efficacy. Intraventricular infusion at the indicated concentrations (A) or at 110 or 460 μg/kg/day (B) was initiated at day 42 postinoculation (A) or at the indicated times (B) in intracerebrally 263K-infected Tg7 mice. *1, $P <$ 0.01 versus the other groups; *2, $P < 0.01$ versus the other groups except the neighboring group(s); *3, $P < 0.05$ versus the control; *4, $P < 0.05$ versus the neighboring group and $P < 0.01$ versus the other groups; *5, $P < 0.01$ versus the control; #, $P < 0.01$.

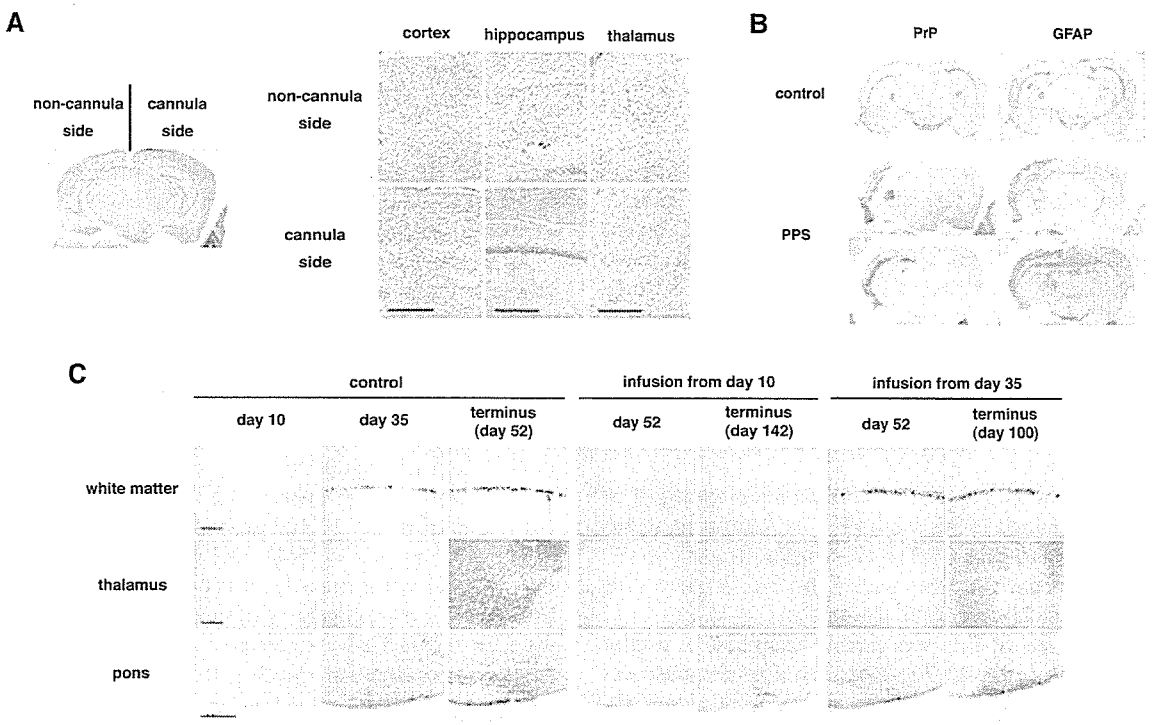

FIG. 3. Histopathology of the brain with or without PPS treatment. (A) Histology of the brain from an intracerebrally 263K-infected, long-surviving mouse treated with PPS at 460 μg/kg/day from day 10 postinoculation. Noncannula side and cannula side represent the sides of pathogen inoculation and intraventricular cannula implantation, respectively. Hematoxylin-eosin staining was used. (B) Immunohistochemical detection of abnormal PrP deposition (PrP) and of neurodegenerative changes by means of glial reaction (GFAP) in the same brain as for panel A (PPS) or in the brain from a nontreated mouse (control). The orientation of the sides of pathogen inoculation and cannula implantation is the same as in panel A. A coronal section sited around one-third of the distance from the interaural line to the bregma line is shown for the control mouse, and either a coronal section sited around one-third of the distance or a coronal section sited around two-thirds of the distance from the interaural line to the bregma line is shown for the PPS-treated mouse. Astrocytic glial reaction is demonstrated by immunohistochemistry for GFAP. (C) Sequential analysis of abnormal PrP deposition in intracerebrally 263K-infected, nontreated mice (control) or mice treated with PPS (infusion from day 10 or 35). Each panel shows a representative finding from three mice sacrificed at a designated time. In PPS-treated mice, the brain tissue examined was obtained from the hemisphere implanted with the intraventricular cannula, which was the hemisphere opposite to that of the inoculation site. PPS was infused at 460 μg/kg/day from day 10 or 35 postinoculation. Each image of the hippocampus or the thalamus (posterior nuclei) is from coronal sections sited around one-third of the distance from the interaural line to the bregma line. Each image of the pons (ventral area) is from a coronal section which is parallel to the interaural line and contains the culmen portion of the cerebellum. Bar, 160 μm.

Safety assessment of PPS. After reference to the Japanese national guidelines for safety studies on medicinal products (rodent and nonrodent toxicity testing), continuous 2-month PPS infusions ranging from 110 to 460 μg/kg/day were performed on each of four to seven adult mongrel dogs, Wistar rats, and Tg7 mice, using an Alzet osmotic pump and a brain infusion cannula. The blood cell count, coagulation, and serum chemistry were analyzed before PPS infusion was initiated and then each month thereafter. An electroencephalogram and 48-h spontaneous activity were recorded for the rats every 2 weeks from the time PPS infusion was started. Animals were sacrificed under deep anesthesia for histological evaluation of the brain when they reached an incurable condition or after the infusion had finished. Animal handling and sacrifice were in accordance with the national prescribed guidelines, and ethical approval for the studies was granted by the Animal Experiment Committee of Kyushu University.

Statistical analysis. Statistical significance was analyzed by repeated-measure analysis of variance followed by Scheffé's method for multiple comparisons.

RESULTS

Vehicle control. Inoculation-related accidental death occurred within 1 week of postintracerebral inoculation and abnormal PrP deposition in the brain appeared at around day 35 postinoculation in Tg7 mice intracerebrally inoculated with 1% 263K homogenate. Accordingly, intraventricular infusion of a chemical was initiated either at an early stage (day 10) or at a late stage (day 35) of the infection in Tg7 mice. Continuous 4-week intraventricular infusion with vehicle alone from day 10 or 35 did not alter the mean incubation time (distilled water, 51.6 ± 1.8 days [n = 5] from day 10 and 51.0 ± 1.8 days [n = 5] from day 35; 25% dimethyl sulfoxide, 52.3 ± 2.1 days [n = 5] from day 10 and 51.2 ± 1.3 days [n = 5] from day 35; untreated, 51.8 ± 2.2 days [n = 8]).

Antimalarial drugs, cysteine protease inhibitor, and amphotericin B. Quinacrine (Fig. 1A), chloroquine (data not shown), and the E-64d cysteine protease inhibitor (data not shown) gave no prolongation effects. Overdose of quinacrine at more than 5 μmol/kg/day from day 10, however, caused adverse effects and shortened the incubation period. Amphotericin B prolonged the incubation time at a dose of 9 or 90 μg/kg/day from day 10 and gave about 26% prolongation of the mean incubation time (from 51 to 64 days) (Fig. 1B). With infusion from day 35, however, no significant prolongation was observed.

PPS. PPS showed the greatest beneficial effects among all of the chemicals examined in this study (Fig. 1C). Infusion at 460 μg/kg/day from day 10 gave 141% prolongation (from 51 to 123 days), and even from the late stage (day 35), it gave 71% prolongation (from 51 days to 87 days).

The dose response of PPS was further examined at a later stage of the infection, day 42 (Fig. 2A). The dose response was in a bell-shaped distribution, and the maximal effect was observed at a dose of 230 μg/kg/day, when the mean incubation time was prolonged by 29% (from 49 to 63 days).

The influence of infusion laterality on the outcome was examined by either ipsilateral or contralateral PPS administration to the inoculation site from day 10 or 35 postinoculation, but no significant difference according to the side of the infusion was observed (data not shown).

The relationship between the infusion initiation time and the outcome was analyzed (Fig. 2B). The effects of PPS were inversely correlated with time after inoculation. High-dose PPS infusion (460 μg/kg/day) at day 7 postinoculation prolonged the mean incubation period by 160% (from 47 to 122 days),

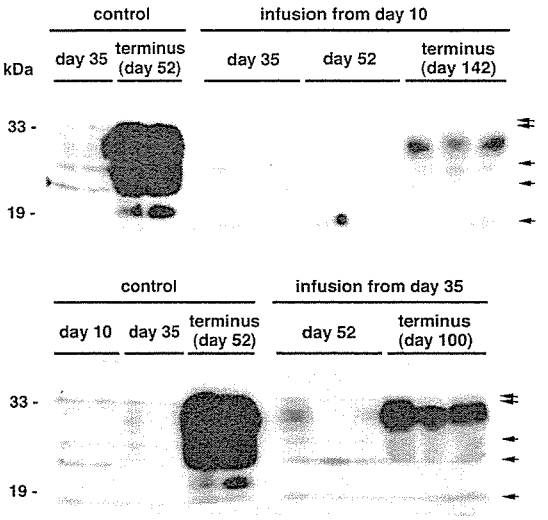

FIG. 4. PrPres in the brain with or without PPS treatment. Each lane represents an aliquot corresponding to 2.0 mg of brain tissue homogenate from an individual mouse sacrificed at a designated time. The brain tissue homogenate examined was prepared from the whole hemisphere contralateral to that of the inoculation site in either nontreated mice (control) or PPS-treated mice (infusion from day 10 or 35). In PPS-treated mice, the brain hemisphere examined was the side implanted with the intraventricular cannula. PPS was infused at 460 μg/kg/day from day 10 or 35 postinoculation. Nonspecific signals that were observed without the primary antibody are shown by arrows.

while that at day 21 postinoculation prolonged it by 106% (from 47 to 97 days). Low-dose PPS infusion (110 μg/kg/day) showed a similar pattern but was less effective.

As a supplementary experiment to compare the efficacy of intraventricular administration with that of peripheral administration, 4-week continuous PPS infusion at 0.2, 2 or 20 mg/kg/day into a subcutaneous area of the back was performed with an osmotic pump from day 10 or 35 postinoculation. None of these treatments yielded any statistically significant effectiveness in prolonging the incubation time (51.0 ± 1.8 days [n = 4], 52.1 ± 2.1 days [n = 4], 52.3 ± 1.6 days [n = 5], and 23.8 ± 16.5 days [n = 5] in the mice receiving 0, 0.2, 2, and 20 mg/kg/day from day 10, respectively; 51.8 ± 2.0 days [n = 4], 51.0 ± 1.8 days [n = 4], 50.0 ± 1.3 days [n = 5], and 40.4 ± 4.3 days [n = 5] in the mice receiving 0, 0.2, 2, and 20 mg/kg/day from day 35, respectively). However, treatment with the highest dose showed adverse effects, such as hemorrhage in the subcutaneous area surrounding the osmotic pump in 80% of the mice examined.

PrP deposition and pathology. Modification of abnormal PrP deposition and pathology in the brains of PPS-treated mice were analyzed (Fig. 3A and B). In the PPS-treated mice with an incubation period of 142 days, the brain hemisphere implanted with the PPS infusion cannula showed very faint or mild pathological changes, whereas the contralateral brain hemisphere was microscopically atrophied and accompanied by prominent spongiform degeneration and neuronal cell loss, especially in the cerebral cortex, hippocampus, and thalamus (Fig. 3A). Similarly, abnormal PrP deposition was prominently reduced within the brain hemisphere implanted with the infusion cannula, while abnormal PrP deposition was much en-

TABLE 1. Infectious titer and incubation time in the 263K-Tg7 model

Dilution	Mean incubation time[a] (days) ± SD	No. of diseased mice/total	Infectious titer[b] (log LD_{50}/20 μl of tissue)	Corrected titer (log LD_{50}/g of tissue)
10^1	43.8 ± 2.5	9/9	6.3	8.0
10^2	48.4 ± 3.1	10/10	5.3	7.0
10^3	55.6 ± 5.3	9/9	4.3	6.0
10^4	65.1 ± 2.9	8/8	3.3	5.0
10^5	76.0 ± 5.3	8/8	2.3	4.0
10^6	93.9 ± 17.0	10/10	1.3	3.0
10^7	158, 177, 422, 443	4/8	0.3	2.0
10^8	338, 555	2/7		
10^9		0/9		

[a] A 20-μl aliquot of serially diluted homogenate samples of the whole brain from a 263K-infected, terminally diseased Tg7 mouse was inoculated intracerebrally into Tg7 mice, and the mice were observed for up to 730 days postinoculation.
[b] The infectious titer was calculated by the Behrens-Kärber method.

hanced within the contralateral hemisphere, compared to the control mice with an incubation period of 52 days (Fig. 3B). GFAP immunoreactivity, indicating glial reaction, was similar to the PrP deposition.

In a sequential analysis of the control mice, cerebral PrP deposition had not appeared at day 10, first appeared in the cerebral white matter adjacent to the hippocampus at around day 35 in a coarse granular deposition pattern, and finally appeared in the thalamus, hypothalamus, and brain stem at terminus day 52 in a punctate pattern (Fig. 3C). Mice treated with PPS from day 10 did not show any PrP deposition within the hemisphere implanted with the cannula at day 52, and only punctate PrP deposition was observed in the brain stem at terminus day 142. Mice treated with PPS from day 35 demonstrated coarse granular PrP deposits in the cerebral white matter at day 52 within the cannula-implanted hemisphere, but there was no apparent PrP deposition in the thalamus at this stage. This PrP deposition pattern was similar to that in the control mice at day 35. Punctate PrP deposition was finally clearly visible in both the thalamus and the brain stem at terminus day 100.

PrPres and infectivity. PrPres was analyzed within the brain hemisphere implanted with the infusion cannula (Fig. 4). PrPres signals in the control mice were very faint at day 35 but ultimately were very strong at terminus day 52. In mice treated with PPS from day 10, PrPres signals were not detected in the brain at day 35 or 52 but were detected at terminus day 142. However, the PrPres signals at day 142 did not reach the high level seen in the control mice at day 52. Similarly, in mice treated with PPS from day 35, the PrPres signals were very weak at day 52 and then increased at terminus day 100, but they still remained at a lower level than in the control mice.

Modification of the infectivity within the brain hemisphere implanted with the infusion cannula was clearly correlated with the level of PrPres (Tables 1 and 2). The infectious titer (log 50% lethal dose [LD_{50}]/g of tissue) within the cannula-implanted brain hemisphere from terminally diseased mice was significantly decreased in the PPS-treated mice.

PPS effects in other strains. To investigate the effectiveness of PPS on pathogen strains other than 263K scrapie agent, Tga20 mice intracerebrally infected with 1% homogenates of RML scrapie agent or Fukuoka-1 Gerstmann-Sträussler-Scheinker disease agent were treated with a dose of 230 μg/kg/day for 4 weeks (Fig. 5). RML-infected mice treated with vehicle alone had a mean incubation period of 65 days, while those treated with PPS from day 14 or 49 postinoculation had a mean incubation period of 141 days (117% prolongation) or 95 days (46%), respectively. Similarly, Fukuoka-1-infected mice had a mean incubation period of 106 days, while those treated with PPS from day 14 or 49 postinoculation had a mean incubation period of 153 days (44% prolongation) or 133 days (25%), respectively. These data imply that intraventricular PPS infusion can be effective irrespective of the pathogen strain.

Safety assessment of intraventricular PPS. Thrombocytopenia and coagulation abnormality are known to occur occasionally with PPS, and PPS has been utilized in humans enterally, percutaneously, or intravenously but never intraventricularly. Thus, the safety of continuous intraventricular infusion should be evaluated before the possibility of application of this specific treatment to human patients is discussed. Continuous intraventricular infusion at doses ranging from 110 to 460 μg/kg/day was examined for 2 months in rodents (mice and rats) and nonrodents (dogs). Intraventricular infusion of up to

TABLE 2. Infectious titer in the brain with PPS treatment

Inoculum[a]	Mouse no.	Mean incubation time[b] (days) ± SD	Infectious titer[c] (log LD_{50}/g of tissue)	Mean infectious titer ± SD[d]
Control	1	56.4 ± 0.5	8.9	8.87 ± 0.06*
	2	56.4 ± 1.6	8.9	
	3	57.2 ± 1.9	8.8	
PPS from:				
Day 35 postinoculation	1	62.4 ± 1.2	8.3	8.20 ± 0.10*
	2	63.4 ± 0.8	8.2	
	3	64.2 ± 5.6	8.1	
Day 10 postinoculation	1	69.8 ± 1.6	7.6	7.50 ± 0.14*
	2	71.4 ± 1.5	7.4	

[a] A 20-μl aliquot of a 0.1% homogenate from the infusion cannula-implanted brain hemisphere of each terminally diseased mouse was used for intracerebral inoculation into Tg7 mice.
[b] The data were collected from five inoculated mice in each group.
[c] The infectious titer was calculated from the incubation period based on the curve obtained from the data in Table 1 and corrected for the dilution power.
[d] *, $P < 0.01$ versus the other groups.

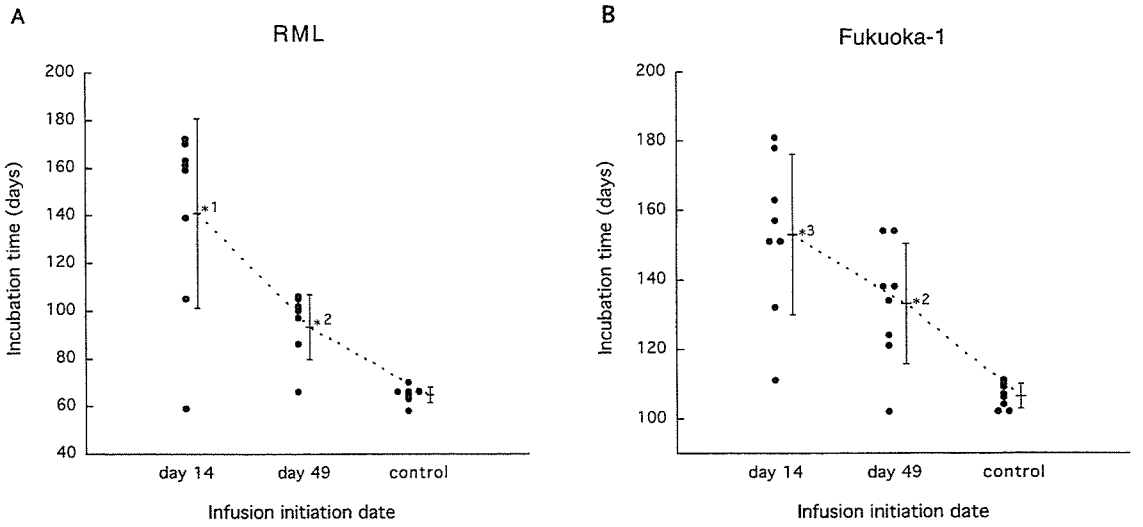

FIG. 5. Efficacy of PPS in mice infected with RML agent (A) or Fukuoka-1 agent (B). PPS at a dose of 230 μg/kg/day was intraventricularly infused into intracerebrally infected Tga20 mice from day 14 or 49 postinoculation for 4 weeks. *1, $P < 0.01$ versus the other groups; *2, $P < 0.05$ versus the control; *3, $P < 0.01$ versus the control.

230 μg/kg/day did not influence the data for the blood cell count, coagulation (Fig. 6), or serum chemistry, nor did it influence the electroencephalogram records, spontaneous activity pattern, behavior, or histological findings for the brain. However, higher doses showed adverse effects, but only in dogs. Three of the six dogs receiving 345 μg/kg/day and all four dogs receiving 460 μg/kg/day suffered partial or generalized seizures, which began within 24 h after PPS infusion was initiated. After treatment with anticonvulsants, the seizures of one dog from each group disappeared. The remaining five dogs did not recover from the seizures. Histologically, three of the five dogs had a large hematoma in the cerebral white matter where the cannula had been placed. None of the other dogs showed any notable pathological findings except for localized tissue damage and gliosis around the cannula route (data not shown).

DISCUSSION

Here, we report on the effectiveness of clinically applicable chemicals by using a new drug evaluation system composed of gene-manipulated mice with substantially shorter disease incubation times and a continuous intraventricular infusion device. This system enabled us to evaluate the absolute therapeutic potency of chemicals in vivo within relatively short periods, regardless of their accessibility to the brain. Our observations indicate that two of the chemicals examined were effective in prolonging the incubation periods for intracerebrally infected animals. This suggests that intraventricular drug infusion could improve the prognosis of infected humans.

Among the chemicals examined here, PPS showed the most beneficial effects, and despite a limited infusion period, mice treated with PPS survived long after the infusion ended. Effectiveness was clearly observed even for the infusion at a late stage of infection, when abnormal PrP deposition was already visible in the affected brain. PPS is known to be effective in inhibiting abnormal PrP formation in vitro (5) and/or in prolonging the disease incubation time in vivo (9, 12, 13, 16). However, its effectiveness in vivo has been restricted to administration either before or soon after peripheral infection. Thus, treatment with PPS has been thought of as being preventive only for those individuals with accidental inoculation in the periphery (7). Our observations, however, indicate that intraventricular PPS is in fact quite effective in prolonging the life spans of infected animals, even after abnormal PrP has already accumulated in the brain. The difference between previous observations and ours can be explained by poor or even no accessibility of peripherally administered PPS to the brain, and this is supported by our observation of the ineffectiveness of continuous subcutaneous PPS administration in intracerebrally infected mice.

The present studies revealed that PPS prevented not only new deposition of abnormal PrP but also the accumulation of neurodegeneration and infectivity. These findings suggest that prolongation of the life spans of infected animals by PPS could be due to its direct action on abnormal PrP generation. PPS interferes with the conversion of normal PrP molecules to abnormal ones by competitively binding to the PrP molecules (4, 5) and/or by altering the cellular localization of normal PrP molecules (20). PPS is also known to play a stimulatory role in the conversion of PrP molecules into protease-resistant ones in vitro (22). However, neither stimulatory effects on abnormal PrP accumulation nor acceleration of the disease course was observed in the present in vivo study.

From the histopathological studies, the effectiveness of PPS was clearly observed within the brain hemisphere where the intraventricular cannula was fitted, but not within the other hemisphere, in treated mice that survived long after the infusion had ended. This suggests that the infused PPS persisted around the infusion site and did not diffuse throughout the ventricular system, especially into the contralateral side of the brain. To obtain a much better outcome following PPS admin-

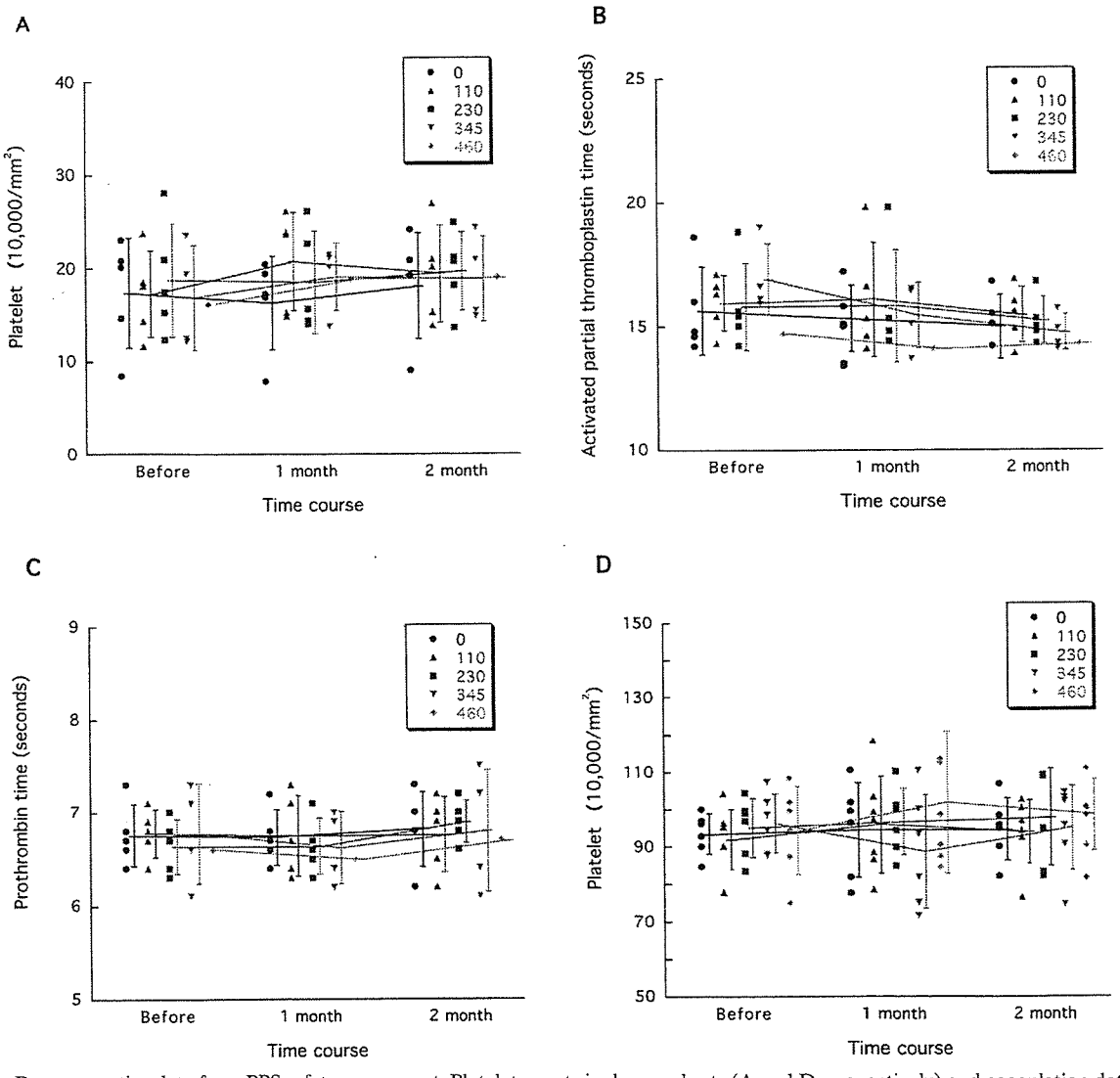

FIG. 6. Representative data from PPS safety assessment. Platelet counts in dogs and rats (A and D, respectively) and coagulation data for dogs (B and C) are shown. Each circle, triangle, square, inverted triangle, or diamond represents an individual animal. The data for two of the six dogs receiving 345 μg/kg/day and for three of the four dogs receiving 460 μg/kg/day were not obtained because they suffered seizures shortly after PPS infusion had been started and were sacrificed or died. However, the data for two dogs, one receiving 345 μg/kg/day and the other receiving 460 μg/kg/day, both of which suffered seizures but recovered, are included.

istration, it may be important to facilitate the diffuse distribution of PPS into every vulnerable area of the brain.

These studies also demonstrated that both the cerebral cortex and the hippocampus were apparently involved in the pathological conditions at the latest stage of the disease in the Tg7-263K model. Coarse granular PrP deposits in the cerebral white matter were the earliest abnormal finding in the affected brain, and these were followed by punctate PrP deposits in the brain stem, hypothalamus, and thalamus, but not in the cerebral cortex and hippocampus, in the nontreated mice. However, mice surviving long after intraventricular PPS infusion had devastating pathological changes in the cerebral cortex and hippocampus of the hemisphere opposite to that of the PPS infusion.

The PPS effects were quite dependent upon the timing of the infusion, and at a later disease stage or a terminal disease stage the effects on prolongation of the life span were substantially limited. We have no precise knowledge as to when the mice used began to exhibit the very initial signs or symptoms of the disease, although we do know that abnormal PrP deposition in the brain began to be visible at around 5 weeks postinoculation and that the mice started to show definite signs about 2 days before death. Thus, our data do not guarantee similar effectiveness in human patients who already have signs and symptoms of the disease. On the other hand, the effectiveness of intraventricular PPS infusion was demonstrated not only for infection with the 263K strain but also for infection with two other distinct strains. These findings suggest that this treatment may have universal validity for TSE diseases.

PPS is utilized as a clinical medicine for interstitial cystitis, thrombophlebitis, and thrombosis, and its safety by enteral, percutaneous or intravenous administration has been clearly

established. Here, the safety of intraventricular PPS infusion at up to a dose yielding the maximal effectiveness in mice was demonstrated in experimental animals. However, at higher doses than this, there was a gap between small rodents and dogs, with the dogs showing adverse effects, such as seizures that were mostly caused by hematoma formation around the intraventricular cannula, although such adverse effects appeared only very early in the treatment. It is well known that smaller animals metabolize drugs much more quickly, and therefore intraventricular PPS at the same dosage was not toxic in mice and rats but was toxic in dogs. For application of this treatment to humans, it will be important to take account of the drug metabolism differences between mice and humans.

Amphotericin B and one of its derivatives are known to prolong the life spans of infected animals even with administration late in the disease course (8). In our experiments, however, amphotericin B did not cause any significant prolongation at a late-stage administration. Differences in the administration route, dose, and duration, as well as the experimental models, might account for this difference, but it remains to be elucidated.

Antimalarial chemicals, including quinacrine, had no effects in the present studies. These chemicals were previously found to be effective in inhibiting abnormal PrP formation in a scrapie-infected cell line (10, 15), and quinacrine has been used in clinical trials for TSE patients. However, together with the recent findings of two other research groups (1, 6), our data suggest that quinacrine may not improve the prognosis of the patients.

Finally, the placement of an intraventricular cannula in TSE patients may create public health issues due to fears of contamination of the operating room or safety issues with respect to the personnel involved with this procedure. For these reasons, other drug delivery systems which do not need a surgical procedure should be developed, and PPS derivatives that can be delivered into the brain after peripheral administration also need to be developed. As an immediately applicable remedy, however, continuous intraventricular PPS administration with an infusion device may be a candidate for a clinical trial, with a view to preventing the disease in those people categorized as being at extremely high risk or to improving the prognosis of diseased people with TSEs.

ACKNOWLEDGMENTS

This study was supported by grants to K.D. from the Ministry of Health, Labour and Welfare (H13-kokoro-025) and from the Ministry of Education, Culture, Sports, Science and Technology (13557118 and 14021085), Tokyo, Japan.

We thank B. Chesebro of the Rocky Mountain Laboratories, National Institute of Allergy and Infectious Diseases, National Institutes of Health, for providing the Tg7 mice and C. Weissmann of the Imperial College School of Medicine at St. Mary's, London, United Kingdom, for providing the Tga20 mice. We also thank I. Goto for the electroencephalogram analyses.

REFERENCES

1. **Barret, A., F. Tagliavini, G. Forloni, C. Bate, M. Salmona, L. Colombo, A. De Luigi, L. Limido, S. Suardi, G. Rossi, F. Auvré, K. T. Adjou, N. Salés, A. Williams, C. Lasmézas, and J. P. Deslys.** 2003. Evaluation of quinacrine treatment for prion diseases. J. Virol. **77**:8462–8469.
2. **Brown, P.** 2002. Drug therapy in human and experimental transmissible spongiform encephalopathy. Neurology **58**:1720–1725.
3. **Brown, P., M. Preece, J. P. Brandel, T. Sato, L. McShane, I. Zerr, A. Fletcher, R. G. Will, M. Pocchiari, N. R. Cashman, J. H. d'Aignaux, L. Cervenakova, J. Fradkin, L. B. Schonberger, and S. J. Collins.** 2000. Iatrogenic Creutzfeldt-Jakob disease at the millennium. Neurology **55**:1075–1081.
4. **Caughey, B., K. Brown, G. J. Raymond, G. E. Katzenstein, and W. Thresher.** 1994. Binding of the protease-sensitive form of PrP (prion protein) to sulfated glycosaminoglycan and Congo red. J. Virol. **68**:2135–2141.
5. **Caughey, B., and G. J. Raymond.** 1993. Sulfated polyanion inhibition of scrapie-associated PrP accumulation in cultured cells. J. Virol. **67**:643–650.
6. **Collins, S. J., V. Lewis, M. Brazier, A. F. Hill, A. Fletcher, and C. L. Masters.** 2002. Quinacrine does not prolong survival in a murine Creutzfeldt-Jakob disease model. Ann. Neurol. **52**:503–506.
7. **Dealler, S.** 1998. Post-exposure prophylaxis after accidental prion inoculation. Lancet **351**:600.
8. **Demaimay, R., K. T. Adjou, V. Beringue, S. Demart, C. I. Lasmézas, J. P. Deslys, M. Seman, and D. Dormont.** 1997. Late treatment with polyene antibiotics can prolong the survival time of scrapie-infected animals. J. Virol. **71**:9685–9689.
9. **Diringer, H., and B. Ehlers.** 1991. Chemoprophylaxis of scrapie in mice. J. Gen. Virol. **72**:457–460.
10. **Doh-ura, K., T. Iwaki, and B. Caughey.** 2000. Lysosomotropic agents and cysteine protease inhibitors inhibit scrapie-associated prion protein accumulation. J. Virol. **74**:4894–4897.
11. **Doh-ura, K., E. Mekada, K. Ogomori, and T. Iwaki.** 2000. Enhanced CD9 expression in the mouse and human brains infected with transmissible spongiform encephalopathies. J. Neuropathol. Exp. Neurol. **59**:774–785.
12. **Ehlers, B., and H. Diringer.** 1984. Dextran sulphate 500 delays and prevents mouse scrapie by impairment of agent replication in spleen. J. Gen. Virol. **65**:1325–1330.
13. **Farquhar, C., A. Dickinson, and M. Bruce.** 1999. Prophylactic potential of pentosan polysulphate in transmissible spongiform encephalopathies. Lancet **353**:117.
14. **Fischer, M., T. Rulicke, A. Raeber, A. Sailer, M. Moser, B. Oesch, S. Brandner, A. Aguzzi, and C. Weissmann.** 1996. Prion protein (PrP) with amino-proximal deletions restoring susceptibility of PrP knockout mice to scrapie. EMBO J. **15**:1255–1264.
15. **Korth, C., B. C. May, F. E. Cohen, and S. B. Prusiner.** 2001. Acridine and phenothiazine derivatives as pharmacotherapeutics for prion disease. Proc. Natl. Acad. Sci. USA **98**:9836–9841.
16. **Ladogana, A., P. Casaccia, L. Ingrosso, M. Cibati, M. Salvatore, Y. G. Xi, C. Masullo, and M. Pocchiari.** 1992. Sulphate polyanions prolong the incubation period of scrapie-infected hamsters. J. Gen. Virol. **73**:661–665.
17. **Priola, S. A., B. Caughey, and W. S. Caughey.** 1999. Novel therapeutic uses for porphyrins and phthalocyanines in the transmissible spongiform encephalopathies. Curr. Opin. Microbiol. **2**:563–566.
18. **Prusiner, S. B.** 1998. Prions. Proc. Natl. Acad. Sci. USA **95**:13363–13383.
19. **Race, R. E., S. A. Priola, R. A. Bessen, D. Ernst, J. Dockter, G. F. Rall, L. Mucke, B. Chesebro, and M. B. Oldstone.** 1995. Neuron-specific expression of a hamster prion protein minigene in transgenic mice induces susceptibility to hamster scrapie agent. Neuron **15**:1183–1191.
20. **Shyng, S. L., S. Lehmann, K. L. Moulder, and D. A. Harris.** 1995. Sulfated glycans stimulate endocytosis of the cellular isoform of the prion protein, PrPC, in cultured cells. J. Biol. Chem. **270**:30221–30229.
21. **Will, R. G., J. W. Ironside, M. Zeidler, S. N. Cousens, K. Estibeiro, A. Alperovitch, S. Poser, M. Pocchiari, A. Hofman, and P. G. Smith.** 1996. A new variant of Creutzfeldt-Jakob disease in the UK. Lancet **347**:921–925.
22. **Wong, C., L. W. Xiong, M. Horiuchi, L. Raymond, K. Wehrly, B. Chesebro, and B. Caughey.** 2001. Sulfated glycans and elevated temperature stimulate PrP(Sc)-dependent cell-free formation of protease-resistant prion protein. EMBO J. **20**:377–386.

Journal of General Virology (2004), 85, 1785–1790 DOI 10.1099/vir.0.19754-0

Amyloid imaging probes are useful for detection of prion plaques and treatment of transmissible spongiform encephalopathies

Kensuke Ishikawa,[1] Katsumi Doh-ura,[1]† Yukitsuka Kudo,[2] Noriyuki Nishida,[3] Ikuko Murakami-Kubo,[1] Yukio Ando,[4] Tohru Sawada[2] and Toru Iwaki[1]

Correspondence
Kensuke Ishikawa
kensuke@np.med.kyushu-u.ac.jp
Katsumi Doh-ura
doh-ura@mail.tains.tohoku.ac.jp

[1]Department of Neuropathology, Neurological Institute, Graduate School of Medical Sciences, Kyushu University, 3-1-1 Maidashi, Higashi-ku, Fukuoka 812-8582, Japan

[2]BF Research Institute Inc., Osaka 565-0873, Japan

[3]Department of Bacteriology, Nagasaki University School of Medicine, Nagasaki, 852-8501, Japan

[4]Department of Laboratory Medicine, Kumamoto University, Kumamoto 860-0081, Japan

Received 24 October 2003
Accepted 2 March 2004

Diagnostic imaging probes have been developed to monitor cerebral amyloid lesions in patients with neurodegenerative disorders. A thioflavin derivative, 2-[4′-(methylamino)phenyl] benzothiazole (BTA-1) and a Congo red derivative, (*trans*, *trans*),-1-bromo-2,5-bis-(3-hydroxycarbonyl-4-hydroxy)styrylbenzene (BSB) are representative chemicals of these probes. In this report, the two chemicals were studied in transmissible spongiform encephalopathies (TSE). Both BTA-1 and BSB selectively bound to compact plaques of prion protein (PrP), not only in the brain specimens of certain types of human TSE, but also in the brains of TSE-infected mice when the probes were injected intravenously. The chemicals bound to plaques in the brains were stable and could be detected for more than 42 h post-injection. In addition, the chemicals inhibited abnormal PrP formation in a cellular model of TSE with IC_{50} values of 4 nM for BTA-1 and 1·4 μM for BSB. In an experimental mouse model, the intravenous injection of 1 mg BSB prolonged the incubation period by 14 %. This efficacy was only observed against the RML strain and not the other strains examined. These observations suggest that these chemicals bind directly to PrP aggregates and inhibit new formation of abnormal PrP in a strain-dependent manner. Both BTA-1 and BSB can be expected to be lead chemicals not only for imaging probes but also for therapeutic drugs for TSEs caused by certain strains.

INTRODUCTION

The transmissible spongiform encephalopathies (TSEs or prion diseases) form a group of fatal neurodegenerative diseases including bovine spongiform encephalopathy, Creutzfeldt–Jakob disease (CJD) and Gerstmann–Sträussler–Scheinker syndrome (GSS). These diseases are characterized by the accumulation in the brain of abnormal protease-resistant isoforms of prion protein (PrP), termed PrP^{Sc} (Prusiner, 1991). The diseases are rare, but outbreaks of acquired forms of CJD, such as variant CJD (Will *et al.*, 1996) and iatrogenic CJD with cadaveric growth hormone or dura grafts (Hamad *et al.*, 2001), have prompted the development of therapeutic interventions and new diagnostic methods.

There are several drug candidates currently under clinical trial for TSE patients, but unfortunately their potential usefulness remains limited. The problem is that these agents can only be given after the onset of the disease, often in the advanced stage, because there is no reliable means of detecting presymptomatic infection by either neuroimaging or laboratory examination. Some studies have reported that imaging assessments such as positron emission tomography (PET) with [^{18}F]FDG and diffusion-weighted magnetic resonance imaging are useful for some types of human TSE (Demaerel *et al.*, 1997; Murata *et al.*, 2002), but are not always conclusive. At present, TSEs can be diagnosed with certainty only through pathological examination or immunoblotting of the diseased brain. Recently, PET and single photon emission CT (SPECT) using radiolabelled imaging probes, which provide information on neuropathological changes as well as brain metabolism, have been reported to be helpful for the early diagnosis of neurodegenerative disorders. A variety of chemicals have been evaluated for imaging β-amyloid (Aβ) aggregation, which is the major

†Present address: Department of Prion Research, Tohoku University Graduate School of Medicine, Sendai 980-8575, Japan.

hallmark of Alzheimer's disease. Candidate probes have primarily been derived from amyloid dyes such as thioflavin and Congo red (Bacskai *et al.*, 2002).

Here, we focused on two candidate probes: a thioflavin derivative, 2-[4′-(methylamino)phenyl] benzothiazole (BTA-1) and a Congo red derivative, (*trans, trans*),-1-bromo-2,5-bis-(3-hydroxycarbonyl-4-hydroxy)styrylbenzene (BSB) (Fig. 1). Both chemicals have been reported to detect amyloid or amyloid-like plaques in either post-mortem human brains or living mouse brains (Mathis *et al.*, 2002; Skovronsky *et al.*, 2000). Since PrP^{Sc} tends to exist as amyloid-like fibrils, we used either BTA-1 or BSB to label PrP deposition in TSE brains. We also examined these chemicals for their application as therapeutics for TSE, since some amyloid-binding chemicals have the potential to inhibit PrP^{Sc} propagation in *in vitro* and/or *in vivo* models of TSE (Supattapone *et al.*, 2002).

METHODS

Chemicals and experimental models. BTA-1 was synthesized at Tanabe R & D (Saitama, Japan), and BSB was kindly provided by Dojindo Laboratories (Kumamoto, Japan). The chemicals were dissolved in 100 % dimethylsulfoxide (DMSO) and stored at 4 °C until use.

Three kinds of TSE-infected mouse neuroblastoma (N2a) cell lines were used in this study: N2a cells infected with the RML strain (ScN2a, Race *et al.*, 1988), N2a#58 cells infected with the 22L strain (L-1, Nishida *et al.*, 2000) and N2a#58 cells infected with the Fukuoka-1 strain (F-3). N2a#58 cells are known to express five times more normal PrP than N2a cells. All cell lines were individually cultured in Opti-MEM (Invitrogen; supplemented with 10 % fetal calf serum).

For *in vivo* studies, transgenic mice models Tg7, over-expressing hamster PrP (Race *et al.*, 1995; Priola *et al.*, 2000), and Tga20, expressing five- to eightfold higher levels of murine PrP (Fischer *et al.*, 1996), were used. These models showed substantially shorter incubation periods following intracranial infection with 20 µl of 1 % (w/v) 263K scrapie strain homogenate and RML strain, respectively. By 6 weeks post-inoculation, the Tg7 mouse model consistently showed plaque-type PrP deposition in the cerebral white matter between the cortex and hippocampus, and at the disease terminal stage showed synaptic-type deposition in the thalamus, hypothalamus and pons. Similarly, the Tga20 mouse model showed plaque-type deposition in the same brain areas, but not as consistently. Permission for the animal study was obtained from the Animal Experiment Committee of Kyushu University. Each mouse weighed approximately 30 g, and was maintained under deep ether anaesthesia during all surgical procedures.

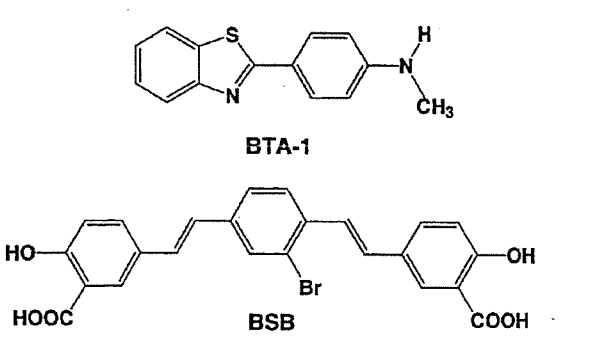

Fig. 1. Structures of the chemicals used in this study.

PrP imaging in pathological sections. Brain samples of autopsy-diagnosed sporadic CJD cases ($n=3$), GSS cases ($n=2$) and non-TSE control cases with amyloid lesions (Alzheimer's disease, $n=2$) or without them (cerebral infarction, $n=1$; pancreatic cancer, $n=1$) were obtained from the Department of Neuropathology, Kyushu University. Tissue samples of TSE material were immersed in 98 % formic acid for 1 h to reduce infectivity. Each tissue sample was embedded in paraffin, and then cut into 7 µm thick sections. Sections of variant CJD brain were kindly provided by James W. Ironside of the CJD Surveillance Unit, Edinburgh, UK. For neuropathological staining, sections were deparaffinized in xylene and hydrated in ethanol. They were then incubated for 30 min in a solution of 1 µM BTA-1 in 50 % ethanol, rinsed and examined under a fluorescent microscope (DMRXA, Leica Instruments) with a UV filter set. The sections were washed overnight in 50 % ethanol. After verifying clearance of the BTA-1 signal, they were incubated for 30 min in a solution of 1 µM BSB and re-examined under the fluorescent microscope. For comparison, each section was subsequently immunostained as described previously (Doh-ura *et al.*, 2000). Briefly, sections were incubated in 0·3 % H_2O_2 in absolute methanol for 30 min and then treated by a hydrolytic autoclave procedure (1 mM HCl, 121 °C, 10 min). After rinsing with 50 mM Tris/HCl, pH 7·6, the sections were incubated at 4 °C overnight with a rabbit primary antibody c-PrP, which was raised against a mouse PrP fragment, amino acids 214–228 (1:200; Immuno-Biological Laboratories, Gunma, Japan) (Yokoyama *et al.*, 2001), followed by incubation with a horseradish-peroxidase-conjugated secondary antibody (1:200; Vector Laboratories) at room temperature for 1 h. The coloured reaction product was developed with 3,3′-diaminobenzidine tetrahydrochloride solution. In addition, formalin-fixed brains of diseased Tg7 mice were investigated using the same procedure. To ensure specificity of the anti-PrP antibody, brain sections with other amyloid lesions such as senile plaques were also immunostained. No positive reactions were obtained.

PrP imaging in presymptomatic mice. BTA-1 or BSB 10–30 mg (kg body weight)$^{-1}$ in 10 % DMSO/saline, or vehicle alone, was administered intravenously into Tg7 mice intracerebrally infected with the 263K strain at 6 weeks post-infection, or into Tga20 mice intracerebrally infected with the RML strain at 8 weeks post-infection. At this point the mice showed no apparent clinical signs of disease. As another control, either chemical was similarly injected into uninfected transgenic mice. The animals were sacrificed at different time-points, and the brains were removed, frozen in powdered dry ice and cut coronally into 10 µm thick sections using a cryostat. The sections were examined under a fluorescent microscope, and then analysed immunohistochemically for PrP as described above.

PrP^{Sc} inhibition in scrapie-infected cells. PrP^{Sc} inhibition assays using a cellular model of TSE were performed as described previously (Caughey & Raymond, 1993). Either BTA-1 or BSB in 100 % DMSO was added at the designated concentrations to each of the cell lines in 6-well plates when they reached 5 % confluency. The final concentration of DMSO in the medium was kept to less than 0·2 %. Two controls, one for untreated cells and the other for cells treated with vehicle alone (0·2 % DMSO), were prepared. The cultures were allowed to grow to confluence, and then harvested and analysed for PrP^{Sc} content by immunoblotting. Briefly, the cells were lysed with lysis buffer (0·5 % sodium deoxycholate, 0·5 % Nonidet P-40, PBS) and digested with 20 µg proteinase K ml^{-1} for 30 min at 37 °C. The digestion was terminated with 0·5 mM phenylmethylsulfonyl fluoride, and the samples were centrifuged at 100 000 *g* for 30 min at 4 °C. Pellets were resuspended in 30 µl of sample loading buffer and boiled for 5 min. The samples were separated on a 15 %

polyacrylamide Tris/glycine SDS gel and transferred to a PVDF filter (Millipore). PrP^{Sc} was detected using a rabbit polyclonal antibody PrP-2B, which was raised against a mouse/hamster PrP fragment, amino acids 89–103 (1:5000) (Murakami-Kubo *et al.*, 2004), followed by an alkaline phosphatase-conjugated goat anti-rabbit antibody (1:20 000; Promega). Immunoreactive signals were visualized using the CDP-Star detection reagent (Amersham) and analysed densitometrically using image analysis software. More than two independent assays were performed for each experiment.

Therapeutic treatment in model animals. BSB dissolved in 10 % DMSO/saline at 1 mg per injection was given intravenously to infected Tg7 mice ($n=5$ in each group) or infected Tga20 mice ($n=7$ in each group). The treatment was performed for Tg7 mice at 35 days post-infection (p.i.) and 50 days p.i., and for Tga20 mice at 45 days p.i. and 60 days p.i. Two control groups were prepared for both experimental models: untreated mice and mice treated with vehicle alone. The animals were monitored 5 days a week until the obvious clinical stage was reached, which was the day before or the day of death in Tg7 mice and 4–5 days before death in Tga20 mice. The statistical significance was analysed by one-way ANOVA followed by Scheffé's method for multiple comparisons.

RESULTS

Imaging of PrP deposition *in vitro* and *in vivo*

Imaging of PrP deposition in the brain by BTA-1 or BSB was first examined using histopathological specimens from human TSE cases. Both chemicals fluorescently labelled most of the compact PrP plaques in the cerebellar cortices of GSS cases (Fig. 2a and c). No residual fluorescence of BTA-1 was seen after thorough washing (Fig. 2b). The labelling intensity was stronger in the sections labelled with BSB compared with those labelled with BTA-1, but the size of each plaque detected by BTA-1 was on average larger than that detected by BSB. The plaques were counterstained with an antibody against the C terminus of PrP (Fig. 2d). In the sections from a variant CJD case, dense PrP plaques were detectable by both chemicals, whereas most of the immunopositive PrP deposits, such as fine granular deposits and perivacuolar deposits, were not labelled (Fig. 2e–h). In the

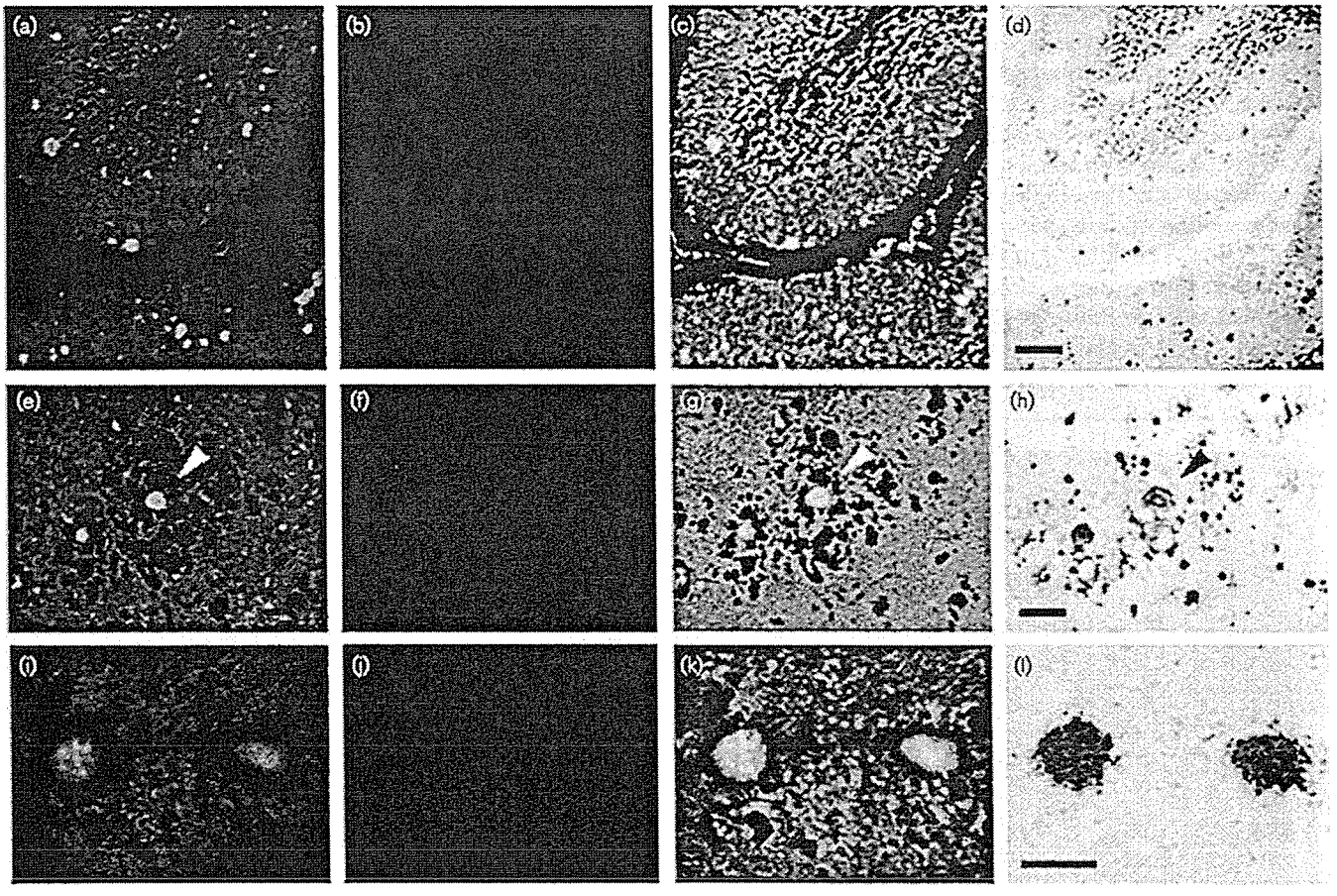

Fig. 2. Imaging of PrP aggregates in brains with TSE. PrP plaques were labelled with BTA-1 (a, e and i); no residual signal was seen after washing to remove BTA-1 (b, f and j). The plaques were then labelled with BSB (c, g and k), and subsequently immunostained for PrP (d, h and l). The first row shows a cerebellar section from a GSS case (a–d), the second shows a cerebral cortical section from a variant CJD case (e–h) and the third shows cerebral white matter section from a terminal Tg7 mouse (i–l). Only dense plaques are identified in the variant CJD section; the arrowheads point to the same PrP plaque. In the Tg7 section, PrP plaques in the cerebral white matter between the cortex and hippocampus were labelled. Bars, 100 (a–d) and 50 (e–l) μm.